DFT Study of Ethylene Polymerization by Zirconocene−Boron Catalytic Systems. Effect of Counterion on the Kinetics and Mechanism of the Process

Ilya E. Nifant'ev,* Leila Yu. Ustynyuk, and Dmitri N. Laikov

Department of Chemistry, Moscow State University, Moscow 119899, Russia

Received January 29, 2001

The effect of counterion on the kinetics and mechanism of ethylene polymerization by the zirconocene−boron catalytic system was examined using the density functional theory approach. A comparative study of three model catalytic species, namely, ethylzirconocene cation, Cp_2ZrEt^+, and two ion pairs of composition $Cp_2ZrEt^+A^-$ ($A^- = CH_3B(C_6F_5)_3^-$, $B(C_6F_5)_4^-$) was carried out. It was shown that the nature of counterion affects mainly the ratio between the most stable β-agostic and nonagostic $Cp_2ZrEt^+A^-$ isomers, the thermodynamic and kinetic characteristics of ethylene addition to the $Cp_2ZrEt^+A^-$ ion pairs, and the chain propagation kinetics. The weaker the nucleophilicity of the counterion, the higher the fraction of the β-agostic isomer, the higher the exotermicity, and the lower the activation barrier to ethylene addition to $Cp_2ZrEt^+A^-$, and the lower the activation energy of chain propagation. All possible pathways of the interaction between $Cp_2ZrEt^+CH_3B(C_6F_5)_3^-$ and ethylene molecule were examined and compared. Among all species of composition $Cp_2ZrEt^+CH_3B(C_6F_5)_3^-$, the nonagostic isomer was found to be the most reactive toward ethylene.

Introduction

Metallocene catalysts of alkene polymerization,[1] which came up to replace the classical Ziegler−Natta systems, have recently attracted considerable interest from quantum chemists.[2] Theoretical studies of the structure and reactivity of metallocene catalysts started by Hoffman and Lauher[3] and followed by Jolly,[4] Morokuma,[5] Fusco,[6] Ziegler,[7] Marks,[8] Brintzinger,[9] Rytter,[10] and other researchers[11−13] have opened the ways for rationalization of unique catalytic properties of these compounds and for prediction of their catalytic activity.

Currently, it is commonly accepted that a species catalyzing polymerization of terminal alkenes is an ion pair composed of alkylzirconocene cation (here, by alkyl is meant the growing polymer chain) and a *weak nucleophilic* anion A^-:[3]

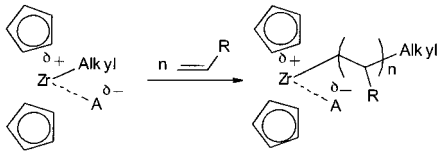

Usually, active catalytic species are generated by the reaction of zirconocene dichloride with large excess of methylalumoxane (in this case, the anion A^- is an

* Corresponding author. E-mail: inif@org.chem.msu.ru.

(1) For review of metallocene-catalyzed alkene polymerization, see: (a) Resconi, L.; Cavallo, L.; Fait, A.; Piemontesi, F. *Chem. Rev.* **2000**, *100*, 1253. (b) Brintzinger, H. H.; Fisher, D.; Mulhaupt, R.; Rieger, B.; Waymouth, R. M. *Angew. Chem., Int. Ed. Engl.* **1995**, *34*, 1143. (c) Bochmannn, M. *J. Chem. Soc., Dalton Trans.* **1996**, 255. (d) Kaminsky, W. *J. Chem. Soc., Dalton Trans.* **1998**, 1413.

(2) Niu, Sh.; Hall, M. B.*Chem. Rev.* **2000**, *100*, 353.

(3) Lauher, J. W.; Hoffmann, R. *J. Am. Chem. Soc.* **1976**, *98*, 1729.

(4) Jolly, C. A.; Marynick, D. S. *J. Am. Chem. Soc.* **1989**, *111*, 7968.

(5) (a) Yoshida, T.; Koga, N.; Morokuma, K. *Organometallics* **1995**, *14*, 746. (b) Kawamura-Kuribayashi, H.; Koga, N.; Morokuma, K. *J. Am. Chem. Soc.* **1992**, *114*, 8687. (c) Musaev, D. G.; Froese, R. D. J.; Morokuma, K. *Organometallics* **1998**, *17*, 1850. (d) Vyboishchikov, S. F.; Musaev, D. G.; Froese, R. D. J.; Morokuma K. *Organometallics* **2001**, *20*, 309.

(6) (a) Fusco, R.; Longo, L.; Masi, F.; Garbassi, F. *Macromolecules* **1997**, *30*, 7673. (b) Fusco, R.; Longo, L.; Provo, A.; Masi, F.; Garbassi, F. *Macromol. Rapid Commun.* **1998**, *19*, 257.

(7) (a) Margl, P.; Deng, L.; Ziegler, T. *Organometallics* **1998**, *17*, 933. (b) Margl, P.; Lohrenz, J. C. W.; Ziegler, T.; Blöchl, P. *J. Am. Chem. Soc.* **1996**, *118*, 4434. (c) Lohrenz, J. C. W.; Woo, T. K.; Ziegler, T. *J. Am. Chem. Soc.* **1995**, *117*, 2793. (d) Woo, T. K.; Fan, L.; Ziegler, T. *Organometallics* **1994**, *13*, 2252. (e) Lohrenz, J. C. W.; Woo, T. K.; Fan, L.; Ziegler, T. *J. Organomet. Chem.* **1995**, *497*, 91. (f) Chan, M. S. W.; Vanka, K.; Pye, C. C.; Ziegler, T. *Organometallics* **1999**, *18*, 4624. (g) Vanka, K.; Chan, M. S. W.; Pye, C. C.; Ziegler, T. *Organometallics* **2000**, *10*, 1841. (h) Chan, M. S. W.; Ziegler, T. *Organometallics* **2000**, *24*, 5182.

(8) (a) Lanza, G.; Fragala, I. L.; Marks, T. J. *J. Am. Chem. Soc.* **1998**, *120*, 8257. (b) Lanza, G.; Fragala, I. L.; Marks, T. J. *J. Am. Chem. Soc.* **2000**, *122*, 12764.

(9) Lieber S.; Prosenc, M.-H.; Brintzinger, H.-H. *Organometallics* **2000**, *19*, 377.

(10) (a) Støvneng, J. A.; Rytter, E. *J. Organomet. Chem.* **1996**, *519*, 277. (b) Thorshang, K.; Støvneng, J. A.; Rytter, E.; Ystenes, M. *Macromolecules* **1998**, *31*, 7149. (c) Thorshang K.; Støvneng J. A.; Rytter E. *Macromolecules* **2000**, *33*, 8136.

(11) For a preliminary communication, see: Nifant'ev, I. E.; Ustynyuk, L. Yu.; Laikov, D. N. In *Organometallic Catayst and Olefin Polymerization*; Blom, R., Follestad, A., Rytter, E., Tilset, M., Ystenes, M., Eds.; Springer-Verlag: Berlin, 2001; p 72.

(12) (a) Cavallo, L.; Guerra, G.; Corradini, P. *J. Am. Chem. Soc.* **1998**, *120*, 2428. (b) Cavallo, L.; Guerra, G. *Macromolecules* **1996**, *29*, 2729.

(13) Boero, M.; Parrinello, M.; Terakura, K. *J. Am. Chem. Soc.* **1998**, *120*, 2746.

10.1021/om010067a CCC: $20.00
Publication on Web 11/14/2001

Scheme 1

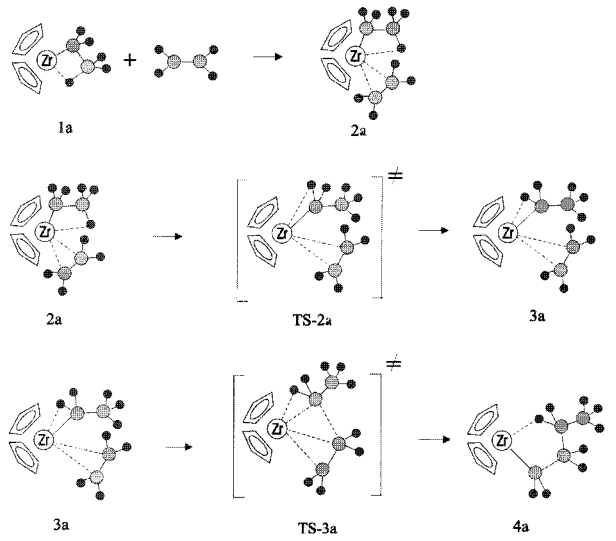

aluminoxane globule with an unknown structure of stoichiometric composition $(AlOMe)_n$) or by the reaction of dimethylzirconocene with either tris(pentafluorophenyl)-boron or $[Ph_3C]^+[B(C_6F_5)_4]^-$ (here, $A^- = Me{-}B(C_6F_5)_3^-$ or $B(C_6F_5)_4^-$, respectively). Weak nucleophilicity of the anion A^- due to both electronic and steric factors allows one to simplify the simulation of polymerization, that is, to consider only the interaction of "*naked*" alkylzirconocene cation with alkene. The growing polymer chain is often represented as ethyl fragment (alkyl = Et). This simplification makes possible (i) a correct consideration of the formation of α- and *β*-agostic bonds, which are of prime importance for polymerization,[14] and (ii) a maximum reduction of both the dimensionality of the problem and the number of structures to be calculated.

Detailed quantum-chemical studies on the mechanism of ethylene polymerization on zirconocene catalysts have been carried out by Ziegler et al.[7a−e] who proposed the mechanism presented in Scheme 1. The ethylzirconocene cation **1a** was used as a model catalytic species. It was shown that the addition of ethylene molecule to **1a** proceeds barrierlessly to give a *β*-agostic adduct **2a** and is accompanied by substantial (∼10 kcal/mol) decrease in the energy of the system. Further isomerization of the *β*-agostic adduct **2a** into α-agostic complex **3a** requires the overcoming of the highest energy barrier **TS-2a** (3.4 kcal/mol according to Ziegler et al.[7c] and 5.2 kcal/mol according to our calculations[15]). Insertion of ethylene molecule into complex **3a** is characterized by very low activation energy and results in *γ*-agostic complex **4a**.

Marks[8] was the first who critically examined the probability of the formation of a separated ion pair taking a model $H_2Si(C_5H_4)(^tBuN)Ti(CH_3)^+CH_3B(C_6F_5)_3^-$ as an example. He showed that the real catalyst is *undeniably* a tight rather than separated ion pair and therefore simulation of alkene polymerization should not be performed ignoring the counterion. This conclusion was also confirmed by Ziegler et al.[7f,g] for zirconocene derived ion pairs.

Fusco[6a] and Bernardi[16] were the first to report a pronounced effect of counterions (Al-containing model compounds) on the energy profiles of the reactions of $L_2TiCH_3^+$ (L = Cl, Cp) with ethylene.

On the other hand, the effect of the nature of counterion on the course of the process remains unclear so far.[17] Besides, no detailed description of all possible intermediates and transition states of ethylene polymerization on zirconocene catalysts (e.g. zirconocene-containing ion pairs) has been reported. Recently, Ziegler et al.[7h] have studied the interaction of ethylene molecule with the $Cp_2ZrEt^+CH_3B(C_6F_5)_3^-$ ion pair. However they have considered only one possible reaction channel. According to the results of our recent calculations[11] and those presented in this work, this channel is not the most energetically favorable. Again, no counterions other than $CH_3B(C_6F_5)_3^-$ were considered in the paper cited.[7h]

We performed a *comparative* study of three model catalytic species, namely, ethylzirconocene cation, Cp_2ZrEt^+, and two ion pairs of composition $Cp_2ZrEt^+A^-$, where $A^- = CH_3B(C_6F_5)_3^-$ and $B(C_6F_5)_4^-$. The systems based on tris(perfluorophenyl)boron were chosen since these ion pairs have been studied in most detail and their structures were established reliably.[18] This differs then from the MAO-containing systems, for which information on the anion structure is lacking and, hence, the models of such systems[6a,b,7g] seem to be hypothetical. It is comparison of the energy profiles of the processes proceeding on ion pairs with different counterions that allowed us to reveal the details of the effect of counterion on the course of alkene polymerization.

The Section "Results and Discussion" presents systematically the following: the description of agostic and nonagostic $Cp_2ZrEt^+A^-$ species and their interconversions; consideration of a polymerization mechanism involving *β*-agostic intermediate **1** (analogously to that proposed earlier by Ziegler et al.[7a−e] for Cp_2ZrEt^+, **1a** (Scheme 1)) for two $Cp_2ZrEt^+A^-$ ion pairs with the counterions $A^- = CH_3B(C_6F_5)_3^-$ and $B(C_6F_5)_4^-$; and consideration of alternative pathways of ethylene addition to various isomeric $Cp_2ZrEt^+CH_3B(C_6F_5)_3^-$ species (compared to the pathway shown in Scheme 1).

The results obtained in this work made it possible to assess the extent to which the nucleophilicity and structure of the anion affect the mechanism and energy profile of the reaction and to propose some ways for targeted modification of catalysts to enhance their activity.

This work was carried out by ignoring solvent effects. Despite the fact that these effects do exist, we believe that *qualitative* consideration of the problem allows us to ignore them. Furthermore, it is well-known that polymerization of ethylene on zirconocene catalysts can proceed in noncoordinating and nonpolar solvents (e.g.,

(14) α-Agostic interactions exert primary control over chain propagation kinetics (Leclerc, M. K.; Brintzinger, H. H. *J. Am. Chem. Soc.* **1995**, *117*, 1651), while *β*-agostic interactions exert primary control over chain termination kinetics (see refs 7c, 10b, and 12b).

(15) Nifant'ev, I. E.; Ustynyuk, L. Yu.; Laikov, D. N. *Russ. Chem. Bull., Int. Ed.* **2000**, *49*, 1164.

(16) Bernardi, F.; Bottoni, A.; Miscione, G. P. *Organometallics* **1998**, *17*, 16.

(17) For review of cocatalysts in metallocene-catalyzed alkene polymerization, see: Chen, E. Y.-X.; Marks, T. J. *Chem. Rev.* **2000**, *100*, 1391.

(18) (a) Yang, X.; Stern, Ch. L.; Marks, T. J. *J. Am. Chem. Soc.* **1994**, *116*, 10015. (b) Jia, L.; Yang, X.; Stern, Ch. L.; Marks, T. J. *Organometallics* **1997**, *16*, 842. (c) Karl, J.; Erker, G.; Frohlich, R. *J. Am. Chem. Soc.* **1997**, *119*, 11165.

hexane) and even in the gas phase. Preliminary results of our study have been reported earlier.[11]

Computational Details

All calculations were carried out using an original program PRIRODA developed by D. N. Laikov.[19] The generalized gradient approximation (GGA) for the exchange-correlation functional by Perdew, Burke, and Ernzerhof[20] was employed. The orbital basis sets of contracted Gaussian-type functions of size (4s)/[2s] for H, (8s4p1d)/[4s2p1d] for C, and (20s16p11d)/[14s11p7d] for Zr were used in conjunction with the density-fitting basis sets of uncontracted Gaussian-type functions of size (4s1p) for H, (7s2p2d) for C, and (22s5p5d4f4g) for Zr.

Full optimization of the geometry of all structures studied in this work was performed using analytical gradients and followed by analytical calculations of the second derivatives of energy with respect to coordinates in order to characterize the nature of the resulting stationary points (minima or saddle points) on the potential energy surface (PES). Zero-point vibrational energies and thermodynamic functions were calculated in the harmonic approximation.

The overall accuracy of these basis set approximations was estimated to be sufficient for the chemical purposes of this work. It is known that the relativistic effects become important for compounds containing 4d transition metals. Nevertheless, they are still quite negligible for the early members, particularly for Zr, due to a cancellation of different relativistic contributions.[21]

In studying the PES of the systems considered we found that there are usually several local energy minima corresponding to structures with slightly different mutual orientation of the cation and anion and conformation of the ethyl or butyl group bound to the Zr atom. We considered all possible structures of each of the intermediates studied and chose the structure with the lowest energy. It is these structures that are discussed in the text below. All other possible structures are, as a rule, not mentioned.

Results and Discussion

(I) Catalytic Species. (A) Isomers of Cp2ZrEt$^+$A$^-$. The model catalytic species studied in this work were the $Cp_2ZrEt^+A^-$ ion pairs with $A^- = CH_3B(C_6F_5)_3^-$ or $B(C_6F_5)_4^-$ and the "naked" ethylzirconocene cation, Cp_2ZrEt^+. Studies of the PES of these systems suggested that the catalytic species can exist in several isomeric forms.

We will begin our consideration with the simplest case, that is, the naked ethylzirconocene cation. The PES of the Cp_2ZrEt^+ system has been studied in detail by Ziegler et al.[7e] It was shown that the ethylzirconocene cation can exist as α- and β-agostic isomeric forms. We optimized the geometries of these complexes (α-agostic complex **5a** and β-agostic complex **1a**). The structures of **1a** and **5a** differ in position of the ethyl fragment with respect to the Cp_2Zr fragment. The free energies, ΔG, of isomers **1a** and **5a** differ by 8.6 kcal/mol (Table 1), which means that the β-agostic isomer **1a** of the ethylzirconocene cation is more thermodynamically stable, which is in agreement with the reported results.[7e]

The number of possible isomeric structures increases from two to four on going from cationic complexes to ion pairs since the anion A^- can be both from the front side and from the backside relative to the Cp_2ZrEt^+ cation. Structures **1b,c** and **6b,c** (Figure 1) are derived from the β-agostic complex **1,** while structures **5b,c** and **5*b,c** (Figure 2) are derived from the α-agostic complex **5**. The energies, thermodynamic characteristics, and selected geometric parameters of these four structures are listed in Table 1.

Table 1. Thermodynamic Data for the Isomers of the Model Catalytic Species $Cp_2ZrEt^+A^-$ and TS of Their Interconversions

	for given param[a]						
	E, kcal/mol	H_{298}, kcal/mol	G_{298}, kcal/mol	Zr−B, Å	Zr−F (C_6F_5), Å		Zr−H (H_3CB), Å
	Naked Cation Cp_2ZrEt^+						
1a	0	0	0				
TS-4a	10.4	9.4	9.2				
5a	10.0	9.3	8.6				
	$A^- = B(C_6F_5)_4^-$						
1b	0	0	0	5.19	2.43	3.36	
TS-4b	6.5	6.5	6.6	5.49	2.48	2.60	
5b	2.0	2.1	0.9	5.37	2.48	2.46	
5b′	1.6	1.8	0.8	5.29	2.57	2.42	
TS-5b	8.5	7.7	7.7	5.17	2.45	3.65	
6b	4.4	4.1	3.9	5.43	2.75	3.88	
	$A^- = CH_3B(C_6F_5)_3^-$						
1c	0	0	0	4.35		2.37	2.61
TS-4c	0.8	0.1	1.0	4.27		2.31	2.53
5c	1.1	1.5	1.7	4.15		2.30	2.35
5c′	1.5	1.9	2.1	4.13		2.30	2.30
TS-5c	3.5	2.5	3.4	4.20		2.29	2.44
6c	2.8	2.6	3.3	4.28		2.31	2.59

[a] The energies (E), enthalpies (H_{298}), and Gibbs free energies (G_{298}) are given relative to the corresponding values for **1**.

The ion pair $Cp_2ZrEt^+A^-$ comprises two weakly bonded fragments and generally a number of local energy minima can correspond to complexes of the types **1b,c**, **5b,c**, **5*b,c**, and **6b,c** on the PES of $Cp_2ZrEt^+A^-$ systems depending on the orientation of the counterion A^- relative to the ethylzirconocene cation. For example, we identified two β-agostic compounds of the type **1** with $A^- = B(C_6F_5)_4^-$. The first of them is the compound described as **1b**. The other compound, **1bb**, is 3 kcal/mol less stable than **1b** and is characterized by longer Zr−B distance compared to **1b** (6.20 vs 5.19 Å, respectively). To avoid multiplication of structures under consideration, in this paper we describe only the most stable isomers of the same type.

If $A^- = CH_3B(C_6F_5)_3^-$, the bridging methyl group can be oriented (rotated) both to the Zr atom and in opposing direction (in this case, the C_6F_5 group is oriented to the Zr atom). The structures belonging to the first type are more thermodynamically stable. This is in agreement with the data of X-ray study,[18a] which confirm this type of orientation of the methyl group.

A salient feature of structures **1b,c** and **6b,c** is the presence of β-agostic bonds. The corresponding C−H bonds are somewhat lengthened as compared to the normal aliphatic bond (1.13−1.17 Å vs 1.10 Å). In both groups of complexes (**1b,c** and **6b,c**), the structure of the Cp_2ZrEt^+ fragment differs appreciably from that of the free ethylzirconocene cation **1a**. These structural distortions are due to the competition between the anion and agostic bond for the coordination sphere of Zr and

(19) Laikov, D. N. *Chem. Phys. Lett.* **1997**, *281*, 151.
(20) Perdew, J. P.; Burke, K.; Ernzerhof, M. *Phys. Rev. Lett.* **1996**, *77*, 3865.
(21) Pyykkö, P. *Chem. Rev.* **1988**, *88*, 563.

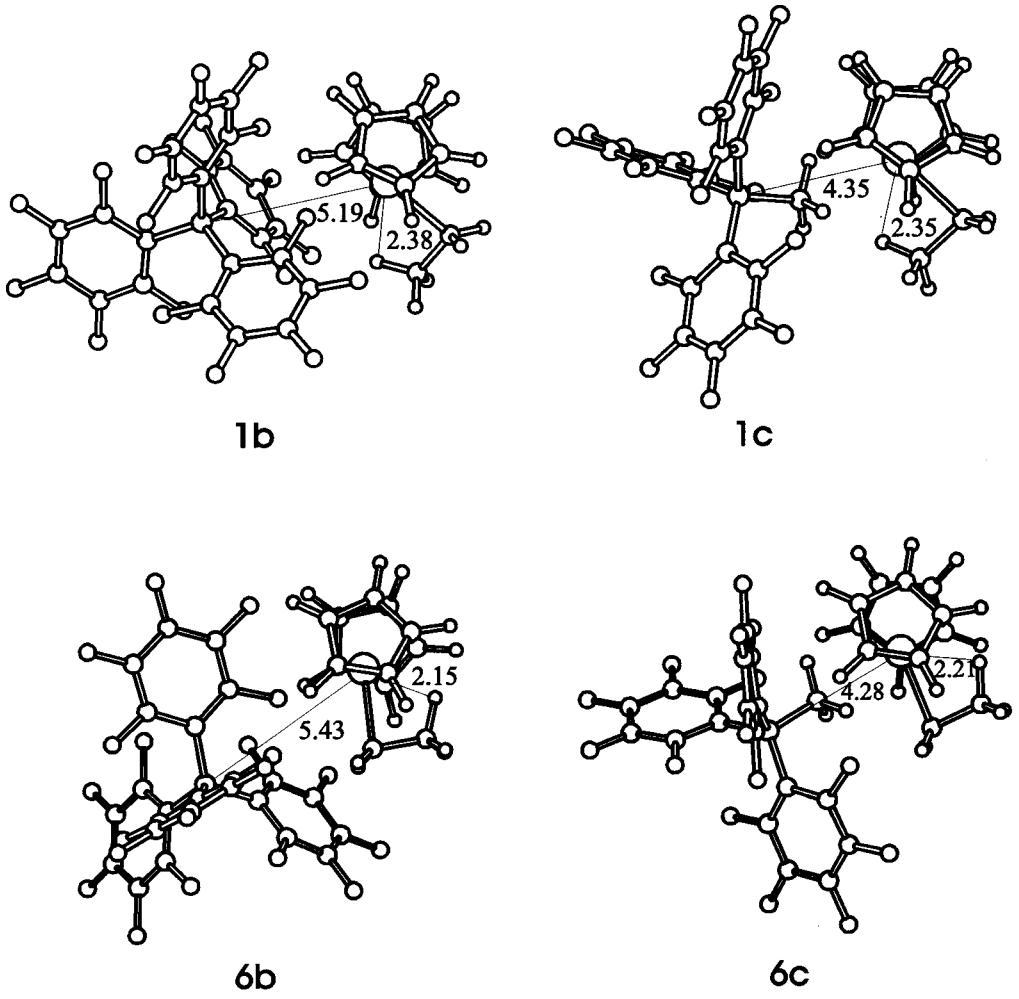

Figure 1. Structures of the ion pairs **1b,c** and **6b,c**.

are most pronounced for the less energetically stable complexes **6b,c**.

A feature of the structures **5b,c** and **5*b,c** (Figure 2) is the absence of agostic interactions. This differs these complexes from the ethylzirconocene cation **5a**. In the isomeric forms **5b,c** and **5*b,c**, all distances from the Zr to H atoms of the ethyl fragment are longer than the sums of the van der Waals radii of these atoms (2.5 Å) and all the C—H bond lengths in the ethyl fragment are equal to the standard aliphatic bond length (1.10 Å). In complex **5a**, the distances between the α-agostic H atom and Zr atom is 2.24 Å, while the corresponding C—H bond length is 1.16 Å. Thus, weak α-agostic bond is cleaved in the presence of the anion.

The energies and Gibbs free energies of the structures **5b,c** and **5*b,c** (Table 1) are very close. These structures can undergo interconversion by rotating about the Zr—C(Et) bond by nearly 120°. Since this interconversion is not accompanied by bond cleavage or formation and the Zr—B distance changes insignificantly, structures **5b,c** and **5*b,c** are simply conformers. We failed to localize the transition states of interconversions between **5b,c** and **5*b,c**. The results of the point-by-point scanning the dependence of the energy of the system on the angle of rotation of the ethyl fragment show that the energy barrier to these interconversions in both cases does not exceed the thermal motion energy at near-room temperatures (0.6 kcal/mol). Therefore, these two conformations are kinetically indistinguishable at higher temperatures, and there is no need to consider them separately. This concerns only unsubstituted zirconocenes and cannot hold for substituted systems, for which both the ratio of the energies of **5b,c** and **5*b,c** and the energy barriers to interconversions can take different values. Among four structures of the $Cp_2ZrEt^+CH_3B(C_6F_5)_3^-$ ion pair studied by Ziegler et al.,[7h] the nonagostic structure similar to isomer **5*** described in the present study also has the lowest energy.

As can be seen from the data listed in Table 1, the nature of anion has a pronounced effect on the relative energies of isomers **1**, **5**, and **6**. If $A^- = CH_3B(C_6F_5)_3^-$, complexes **5c** and **5*c** have the lowest energy. On the other hand, complexes **1** have the lowest energies for $A^- = B(C_6F_5)_4^-$ and for ethylzirconocene cation. This suggests that the anion A^- is in competition with the agostic bond within the coordination sphere of Zr. As a result, the ratio of the energies of the α- and β-agostic ion pairs formed is mainly determined by nucleophilicity of the anion A^-.[22] The higher the nucleophilicity of the anion A^-, the tighter the binding within the

(22) Hereafter, by nucleophilicity of an anion is meant a totality of electronic and steric factors responsible for the ability of the anion to be involved in the interaction with ethylzirconocene cation.

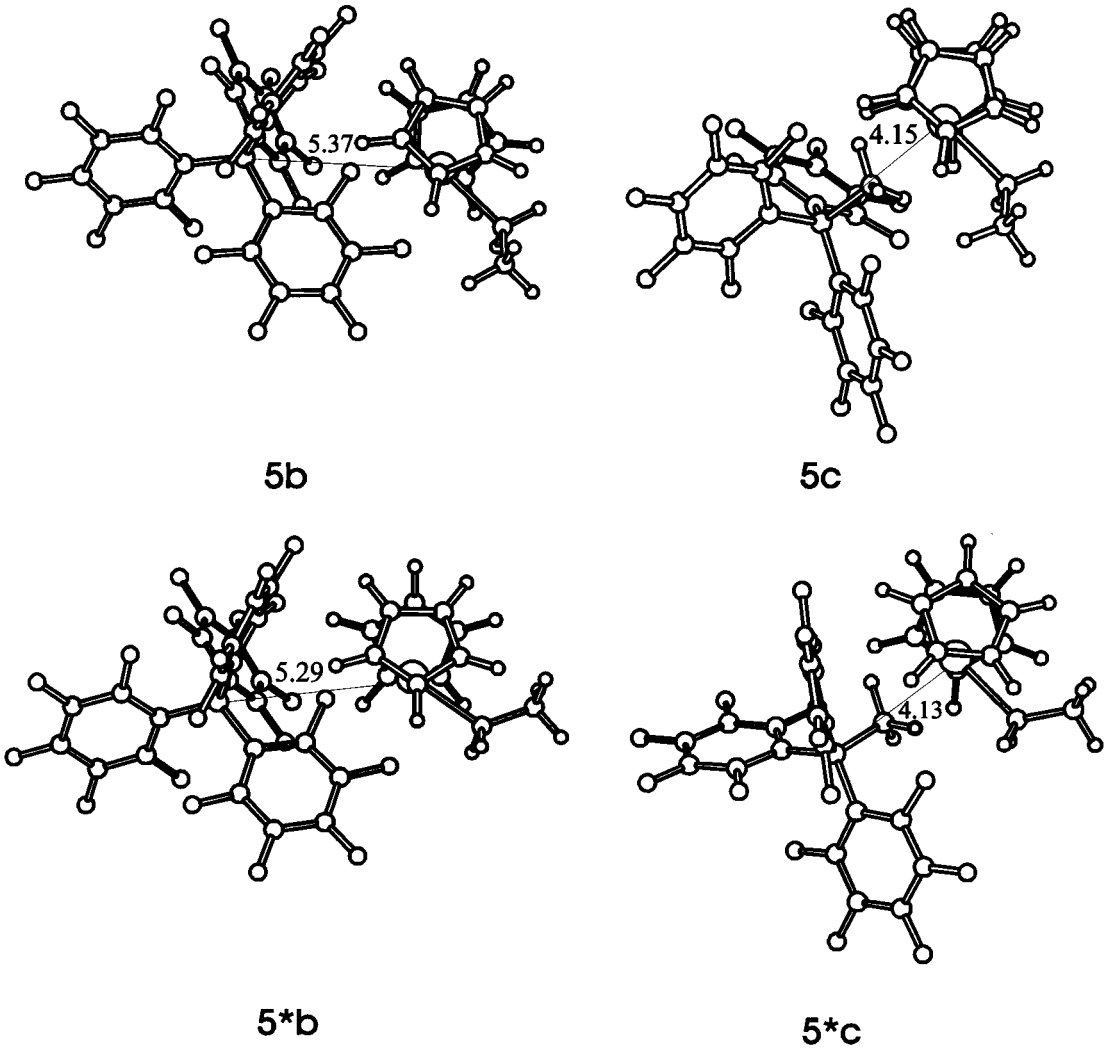

Figure 2. Structures of the ion pairs **5b,c** and **5*b,c**.

coordination sphere of Zr (the shorter the Zr—B distance), the weaker the β-agostic bond, and the higher the energies of β-agostic complexes **1** and **6** relative to that of isomer **5**.

Since, as was mentioned above, the energy of the system is controlled by the interaction between the components of the ion pair, it should be emphasized that this interaction is not purely electrostatic. This is indicated by the short contacts between the zirconium ion and some of the constituent atoms of the anion. For $A^- = B(C_6F_5)_4^-$, at least one Zr—F distance in all optimized structures does not exceed 2.75 Å. A characteristic feature of isomer **5b** is the presence of two such contacts of lengths 2.46 and 2.48 Å. On the other hand there is only one short contact Zr—F in β-agostic complex **1b** (2.43 Å). That is the most probable reason for the slightly different anion orientation in **1b** and **5b** toward the cation and longer Zr—B distances in **5b** in comparison to that in **1b**.

Therefore, fluorine atoms constituting the anion interact with the Zr atom, thus filling the coordination vacancy. This is responsible for the absence of agostic bond in structure **5b** in contrast to **5a**. Indeed, the coordination vacancy in complex **5a** is filled owing to the formation of a weak α-agostic bond, whereas in isomer **5b** this occurs due the interaction with fluorine atoms constituting the anion. Recently, a number of experimental studies on this type of interaction have been reported. For instance, X-ray studies of the structures of several zirconocene complexes with more complex counterions based on $B(C_6F_5)_3$ revealed short Zr—F contacts with one or two F atoms constituting the counterion.[18b,c] The two shortest distances to the F (**b**) or H atoms (**c**) of the methyl group of the anion are listed in Table 1.

Isomer **5c** with $A^- = CH_3B(C_6F_5)_3^-$ is stabilized by the agostic interaction with hydrogen atoms of the CH_3 group. It is the electrons of two C—H bonds of this group that are involved in the filling of the coordination vacancy of the Zr ion.

Thus, our study of the PES of $Cp_2ZrEt^+A^-$ systems with $A^- = CH_3B(C_6F_5)_3^-$ and $B(C_6F_5)_4^-$ showed that the model catalytic species can exist in isomeric forms **1**, **5**, **5***, and **6**, which have close energies and differ in orientation of the ethyl fragment and counterion with respect to Cp_2Zr.

(B) Interconversions of Isomers 1, 5, and 6. The isomers **1**, **5**, and **6** can undergo interconversions. Some of them proceed with formation or cleavage of the agostic bond (interconversions **1** ⇌ **5**), whereas in some instances the agostic bond is retained (interconversions **1** ⇌ **6**). Interconversions **1** ⇌ **5** can occur by rotating

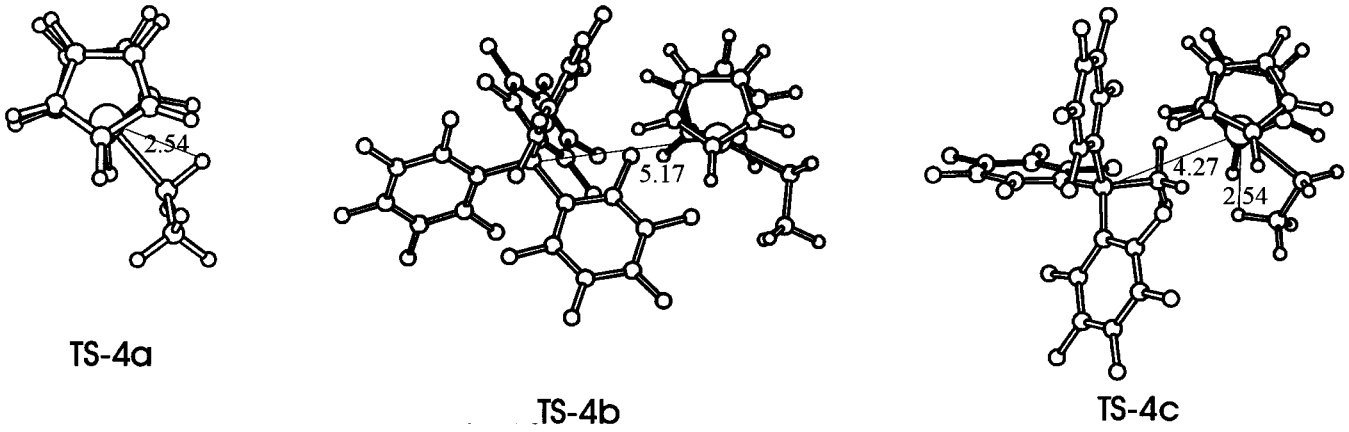

Figure 3. Structures of the transition states **TS-4a**−**c**.

the ethyl fragment about the Zr—C bond by nearly 60° and are accompanied by cleavage of the β-agostic bond:

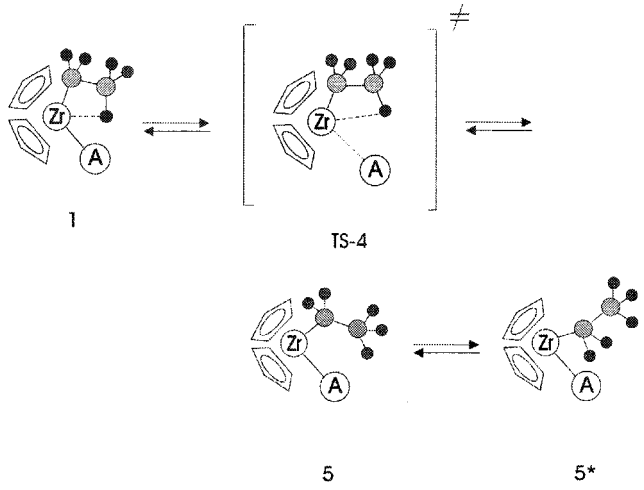

The structures of the transition states of this interconversion are shown in Figure 3 (**TS-4a**−**c**). As can be seen in Figure 3, the geometry of **TS-4** is strongly dependent on the nature of counterion. In the case of "naked" ethylzirconocene cation, the transition state **TS-4a** is near the α-agostic complex **5a** on the reaction coordinate. If $A^- = CH_3B(C_6F_5)_3^-$ (the stronger nucleophile), **TS-4c** is near the β-agostic complex **1c** and if $A^- = B(C_6F_5)_4^-$ (a weaker nucleophile), the geometry of **TS-4b** is intermediate between those of **TS-4a** and **TS-4c**.

The energy diagram shown in Figure 4 illustrates the ratio of the Gibbs free energies, G_{298}, of the structures **1**, **5**, and **6** and the transition states of their interconversions. As can be seen in Figure 4 and from the data listed in Table 1, the ratio of the Gibbs free energies of the isomers **1** and **5**, as well as the height of the energy barrier **TS-4** associated with the cleavage of the β-agostic Zr—H bond, are strongly dependent on the nature of anion: the higher the nucleophilicity of the anion, the lower the energy of isomer **5** and the lower the energy barrier to the cleavage of the β-agostic bond. The free activation energies, $\Delta G_{298}^{\ddagger}$, of the conversion **1** → **5** (see Table 1) are 9.2 kcal/mol for the ethylzirconocene cation (**TS-4a**), 6.6 kcal/mol for $A^- = B(C_6F_5)_4^-$ (**TS-4b**), and 1.0 kcal/mol for $CH_3B(C_6F_5)_3^-$ (**TS-4c**). The differences $\Delta G_{298}^{\ddagger} = G_{298}$(**TS-4**) − G_{298}(**5**) for the reverse process **5** → **1** are 0.6 (**a**), 5.7 (**b**), and 2.5 kcal/mol (**c**). Therefore, the last conversion can be associated with the overcoming of a rather high energy barrier.

Analogously, conversion of complexes **6b,c** into the corresponding complexes **5b,c** occurs with cleavage of the β-agostic bond and is accompanied by rotation of the ethyl fragment about the Zr—C bond:

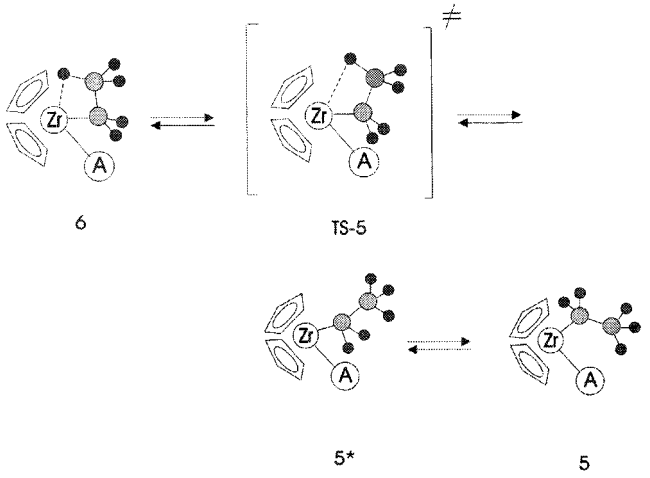

This transformation results in intermediate **5*** as the primary product, which is a conformer of the nonagostic structure of the ion pair (see above) and readily undergoes conversion into **5** by rotating the ethyl fragment about the Zr—C(Et) bond.

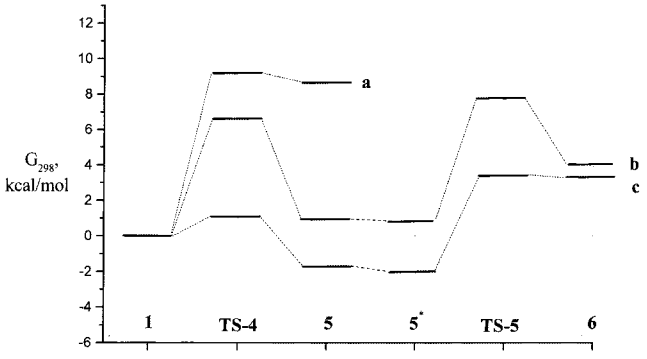

Figure 4. Free energy profile for the interconversion reactions of the complexes **1**, **5**, **5*,** and **6**.

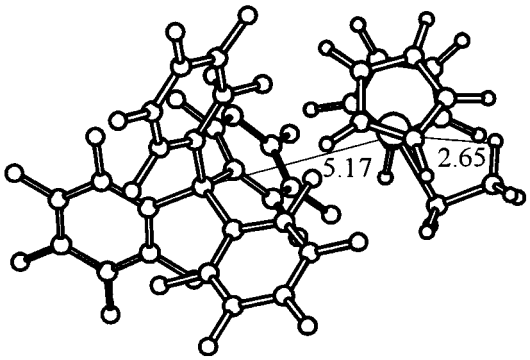

TS-5b

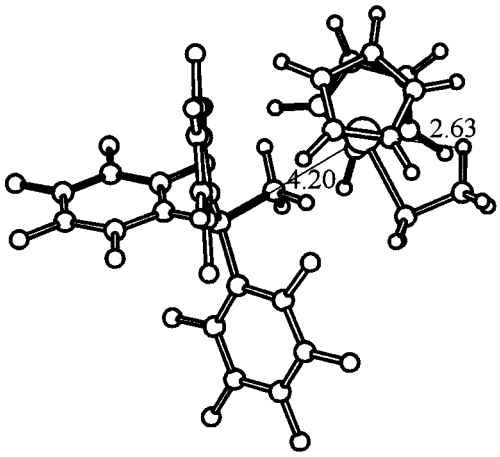

TS-5c

Figure 5. Structures of the transition states **TS-5b,c**.

The structures of the corresponding **TS-5b,c** are shown in Figure 5. In both cases, the transition states of conversion **6b,c** → **5b,c** (**TS-5b,c**) are near the β-agostic complexes (**6b,c**), and the corresponding energy barrier is associated with the cleavage of the β-agostic Zr–H bond. As can be seen in Figure 4, the energy barrier $\Delta G_{298}^{\ddagger} = G_{298}(\mathbf{TS\text{-}5}) - G_{298}(\mathbf{6})$ to conversion **6** → **5** decreases substantially with increasing the nucleophilicity of the anion (3.8 kcal/mol for $A^- = B(C_6F_5)_4^-$ vs 0.1 kcal/mol for $A^- = CH_3B(C_6F_5)_3^-$), so that the conversion **6c** → **5c** proceeds nearly barrierlessly at 298 K. The differences $\Delta G_{298}^{\ddagger} = G_{298}(\mathbf{TS\text{-}5}) - G_{298}(\mathbf{5})$ for the reverse process **5b,c** → **6b,c** are 6.8 (**b**) and 5.1 kcal/mol (**c**).

Interconversion **1** ⇌ **6** can proceed by moving the cation and anion relative to each other; this is also called "reorganization":[23]

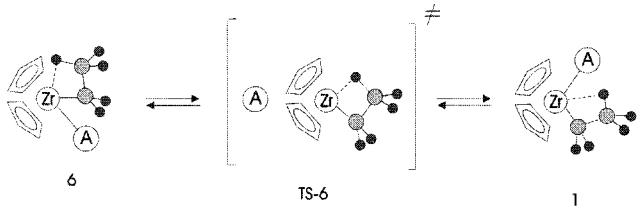

Detailed consideration of this issue, as applied to the mechanism of polymerization on ion pairs, is given in section 4 of part II of this work.

(II) Chain Propagation Step. (A) Transformations of Intermediate 1. (1) Ethylene Addition to Intermediate 1. The interaction of β-agostic isomer of the ethylzirconocene cation Cp_2ZrEt^+ (**1a**) with ethylene molecule has been studied in detail by Ziegler et al.[7a–e] In this work, we considered the interaction of β-agostic isomers of the $Cp_2ZrEt^+A^-$ ion pair (**1b,c**) with ethylene molecule. Scheme 2 illustrates the mechanism of this interaction, which is similar to that proposed for Cp_2ZrEt^+ cation.[7a–e] Out of the two types of β-agostic complexes (**1** and **6**), the most thermodynamically stable isomers **1b,c** were considered as reagents. We optimized the structures of intermediates and transition states of their transformations into the corresponding reaction products **4b,c** and found that the energy profiles of the reactions involving counterions change appreciably as compared to that of the reaction with the Cp_2ZrEt^+ cation.

Scheme 2

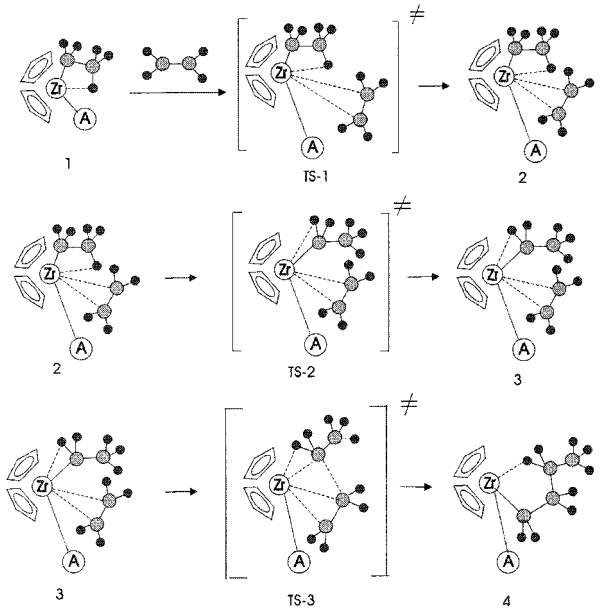

According to our calculations, the addition of ethylene to **1** proceeds through **TS-1**. In contrast to the "naked" cation, not only does the energy barrier to this process exist in the case of model ion pairs $Cp_2ZrEt^+A^-$, but can be rather high. This barrier is first of all due to the fact that the anion A^- is displaced into the outer coordination sphere during the ethylene addition, thus making room for the ethylene molecule within the coordination sphere of the zirconium ion. It was found that, depending on the type of anion, the Zr–B distance increases by ~1.1–1.2 Å in the transition state **TS-1** and by 1.5–2.3 Å in the reaction product **2** as compared to the corresponding distance in the initial complex **1**. The structures of complexes **2** and the transition states **TS-1** of the ethylene addition reaction are shown in Figures 6 and 7, respectively, and their energies and thermodynamic characteristics are listed in Table 2. The

(23) (a) Deck, P. A.; Marks, T. J. *J. Am. Chem. Soc.* **1995**, *117*, 6128. (b) Beswick, C. L.; Marks, T. J. *Organometallics* **1999**, *18*, 2410. (c) Beswick, C. L.; Marks, T. J. *J. Am. Chem. Soc.* **2000**, *122*, 10358.

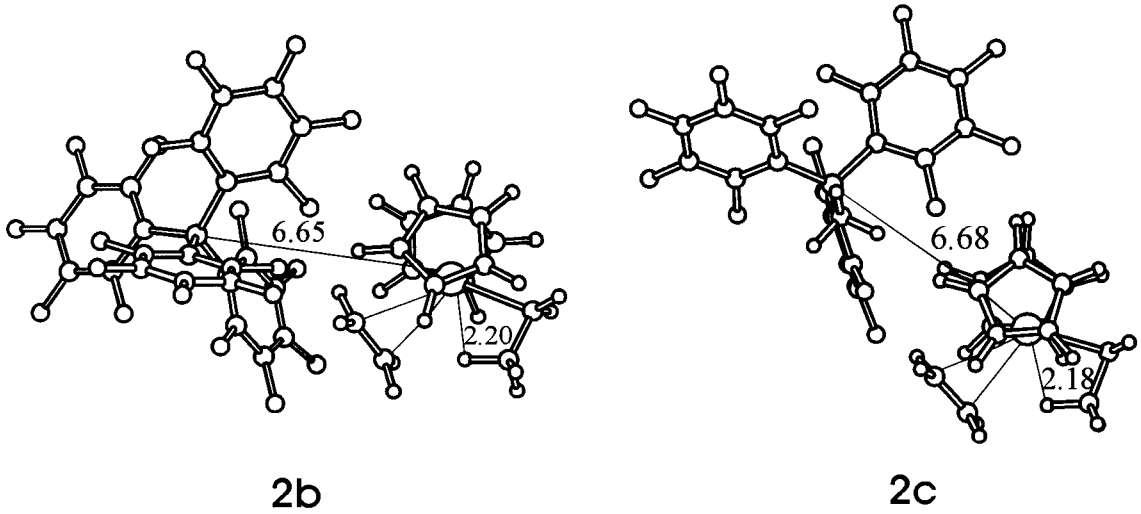

Figure 6. Structures of the complexes **2b,c**.

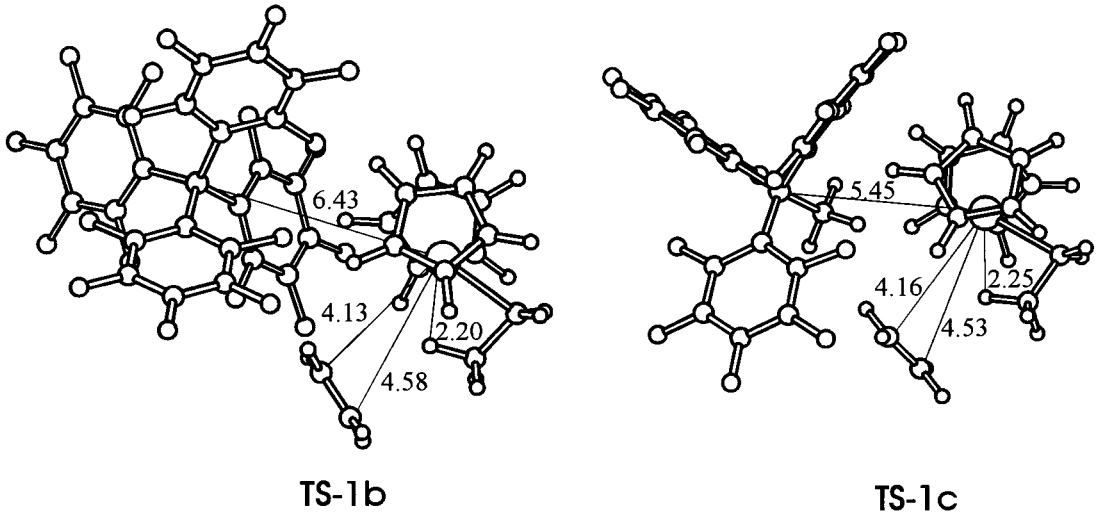

Figure 7. Structures of the transition states **TS-1b,c**.

ethylene molecule deviates slightly from the plane which passes through the Zr atom and is equidistant from the cyclopentadienyl ligands. The distances from the Zr atom to the carbon atoms of the ethylene molecule are somewhat different.

Analysis of the results obtained for all systems under consideration showed that the β-agostic bond in **1** is not only retained in both **TS-1** and addition product **2** during the addition of ethylene molecule to **1**, but is appreciably shortened, thus becoming stronger for the reaction involving the $Cp_2ZrEt^+A^-$ ion pairs. Thus, the function of the β-agostic bond is to provide additional stabilization of the system in the stage of formation of intermediate complex **2** with ethylene molecule.

Yet another salient feature of ethylene addition to $Cp_2ZrEt^+A^-$ ion pairs compared to the addition to the Cp_2ZrEt^+ cation is that the former is less exothermic than the latter due to an increase in the degree of charge separation within the ion pair (an increase in the Zr—B distance). This effect is most pronounced for $A^- = CH_3B(C_6F_5)_3^-$, which is the strongest nucleophile among the counterions studied. As can be seen from the data listed in Table 2, the addition of ethylene molecule to Cp_2ZrEt^+ to give intermediate complex **2** is characterized by the rather large negative value of ΔH_{298} (−14.4 kcal/mol), whereas for the ion pair with $CH_3B(C_6F_5)_3^-$ as the counterion A^- this value is close to zero. The addition of ethylene molecule is also accompanied by considerable loss of entropy of the system, which makes a contribution of more than 10 kcal/mol to the ΔG_{298} value for this reaction (Table 2). Previously, this effect was reported by different authors who studied the addition of ethylene molecule to ethylzirconocene cation.[7c] Comparison of the changes in the ΔS_{298} values for ethylene addition in the systems studied showed that the loss of entropy is maximum for the ethylzirconocene cation, since for other systems it is to a certain extent compensated for by the weakening of the bonding within the ion pair.

The most important results obtained in this part of our study are as follows. First, we found that the height of the energy barrier **TS-1** is determined by the properties of the counterion. It is maximum for the most nucleophilic anion $A^- = CH_3B(C_6F_5)_3^-$ and is zero for the "naked" ethylzirconocene cation (see Table 2). Second, we found that the counterion moves aside with respect to the Zr atom upon the addition of ethylene molecule. This leads to an increase in endothermicity of the reaction and to simultaneous increase in the height of the energy barrier **TS-1**.

Table 2. Thermodynamic Data of the Intermediates and Transition States for the Model Reaction $Cp_2ZrEt^+A^- + C_2H_4 \rightarrow Cp_2ZrBu^+A^-$

	for given param[a]			
	E, kcal/mol	H_{298}, kcal/mol	G_{298}, kcal/mol	Zr−B, Å
	Naked Cation Cp_2ZrEt^+			
1a	0	0	0	
TS-1a				
2a	16.2	14.4	2.0	
TS-2a	10.4	9.8	2.5	
3a	13.6	12.9	0.3	
TS-3a				
4a	31.11	28.3	15.9	
	$A^- = B(C_6F_5)_4^-$			
1b	0	0	0	5.19
TS-1b	0.38	1.4	10.5	6.43
2b	9.6	7.2	3.8	6.65
TS-2b	3.5	2.4	8.7	6.42
3b	4.6	3.3	6.5	6.46
TS-3b	3.8	2.8	9.4	6.35
4b	18.75	16.0	4.9	6.49
	$A^- = CH_3B(C_6F_5)_3^-$			
1c	0	0	0	4.36
TS-1c	10.4	10.6	21.7	5.45
2c	1.0	0.1	11.3	6.68
TS-2c	3.7	3.4	15.1	6.23
3c	2.2	2.6	12.9	6.29
TS-3c	3.1	3.2	15.2	6.23
4c	11.9	9.9	1.50	6.13

[a] Energies (*E*), enthalpies (H_{298}), and Gibbs free energies (G_{298}) are given relative to the corresponding values for noninteracting reagents **1** + C_2H_4.

In addition to the ethylene addition step, the ratio of the energies of the initial agostic and nonagostic complexes **1**, **5**, and **6** and, hence, their relative content in the equilibrium mixture of reagents also appeared to be sensitive to the properties of the counterion. Thus, we found that the reactions of "naked" ethylzirconocene cation and those of ion pairs with ethylene molecule are fundamentally different. Taken together, the aforesaid indicates that correct description of real systems requires the inclusion of anions in the model systems used in theoretical studies on the alkene polymerization on the zirconocene and other metallocene catalysts.

(2) Isomerization of *β*-Agostic Intermediate 2 into α-Agostic Complex 3. Detailed comparison of all reaction stages with the mechanism presented in Scheme 2 shows that, beginning with the second stage, they are to a lesser extent dependent on the nucleophilicity of counterion than the first stage (ethylene addition).

Complexes **2a**−**c** undergo isomerizations into corresponding α-agostic complexes **3a**−**c** through the transition states **TS-2a**−**c**. For the system Cp_2ZrEt^+, this was studied by Ziegler et al.[7a−e] In this work, we optimized the structures of **TS-2a**−**c** and complexes **3a**−**c** for all systems under consideration. They are presented in Figures 8 and 9, respectively, and their energies and thermodynamic characteristics are listed in Table 2. It should be noted that the energy differences between **TS-2a**−**c** and complexes **2a**−**c** depend only slightly on the nature of counterion (cf. 5.8 kcal/mol for the ethylzirconocene cation (**TS-2a**), 6.1 kcal/mol for $B(C_6F_5)_4^-$ (**TS-2b**), and 4.6 kcal/mol for $CH_3B(C_6F_5)_3^-$ (**TS-2c**)). This is likely due to the fact that structural changes during the transformation **2** → **3** occur mainly within the cation, whereas the distance between the anion and cation changes only slightly. Nevertheless, for the three systems studied in this work the energies of **TS-2a**−**c** calculated relative to those of noninteracting reagents (**1a**−**c** + C_2H_4) and listed in Table 3 differ appreciably and increase in the order ethylzirconocene cation < $B(C_6F_5)_4^-$ < $CH_3B(C_6F_5)_3^-$, which is due to an increase in the energies of complexes **2a**−**c** relative to those of noninteracting reagents in the same order.

Table 3. Thermodynamic Data of the Intermediates and Transition States for the Complex 4 Rearrangements Presented in Scheme 3

	for given param[a]			
	E, kcal/mol	H_{298}, kcal/mol	G_{298}, kcal/mol	Zr−B, Å
	Naked Cation Cp_2ZrEt^+			
1a	0	0	0	
4a	31.1	28.3	15.9	
TS-7a	28.7	26.5	13.0	
6′a (1′a)	34.1	32.1	17.5	
	$A^- = B(C_6F_5)_4^-$			
1b	0	0	0	5.19
4b	18.8	16.0	4.9	6.49
7b	31.0	28.6	16.1	5.17
TS-7b	17.4	15.0	3.5	6.46
6′b	28.5	26.5	15.5	5.46
TS-8b	17.2	15.1	2.6	6.54
5′b	30.6	27.8	16.8	5.36
5′*b	32.9	30.7	19.2	5.11
TS-9b	24.8	22.7	11.2	5.66
1′b	32.7	30.0	17.2	5.18
TS-10b	27.4	25.5	13.2	5.18
	$A^- = CH_3B(C_6F_5)_3^-$			
1c	0	0	0	4.36
4c	11.9	9.9	1.5	6.13
7c	32.9	30.6	17.7	4.15
TS-7c	10.6	9.2	3.9	6.56
6′c	29.7	27.7	12.7	4.30
TS-8c	7.3	6.7	3.7	6.10
5′c	35.5	33.1	19.4	4.15
5′*c	33.4	31.1	19.1	4.15
TS-9c	32.5	30.8	16.3	4.14
1′c	33.5	31.0	17.6	4.28
TS-10c	24.7	23.2	9.9	4.13

[a] Energies (*E*), enthalpies (H_{298}), and Gibbs free energies (G_{298}) are given relative to corresponding values for noninteracting reagents **1** + C_2H_4.

Analysis of peculiarities of the geometry of transition states **TS-2b**−**c** showed that the distances to the corresponding hydrogen atoms involved in α-agostic bonding are 2.47 Å for the ion pairs $Cp_2ZrEt^+A^-$ and 2.69 Å for isolated cation. The formation of α-agostic bond leads to an increase in the separation between the anion A^- and Zr atom by 0.4−0.6 Å. This suggests that these transition states are somewhat closer to the reaction products, that is, α-agostic complexes **4b,c**, as compared to isolated ethylzirconocene cation.

(3) Formation of C−C Bond in Intermediate 3. Ethylene insertion into the Zr−C bond through the transition state **TS-3** (Figure 10, Table 2) results in *γ*-agostic complex **4** (Figure 11, Table 2). In the case of cationic complex **3a**, the geometry optimization of **TS-3a** leads to the primary insertion product **4a**, which suggests that the α-agostic complex **3a** and **TS-3a** have very close energies. This was first found by Ziegler et al.[7e] who estimated the energy barrier **TS-3a** (relative to **3a**) at about 0.5 kcal/mol. Our attempt to localize this transition state failed and the structure of the α-agostic

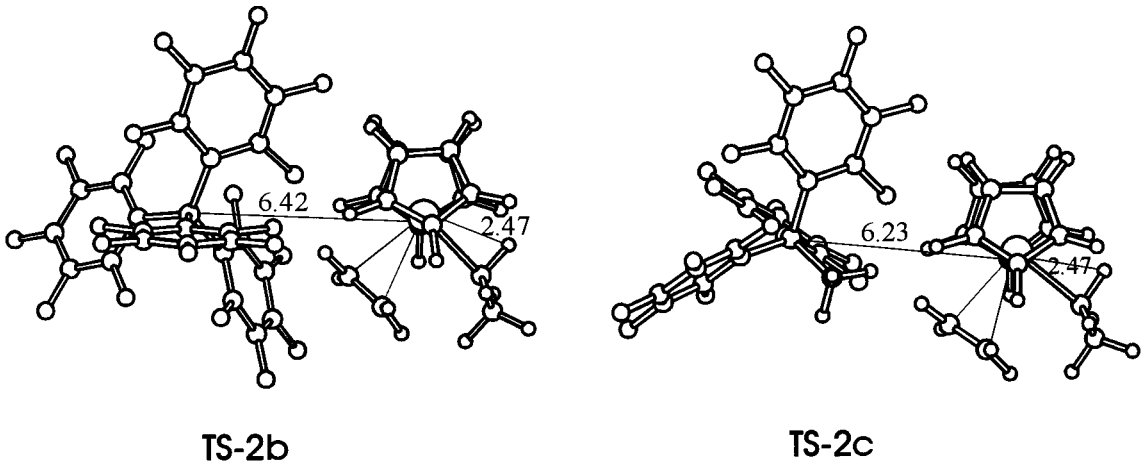

Figure 8. Structures of the transition states **TS-2b,c**.

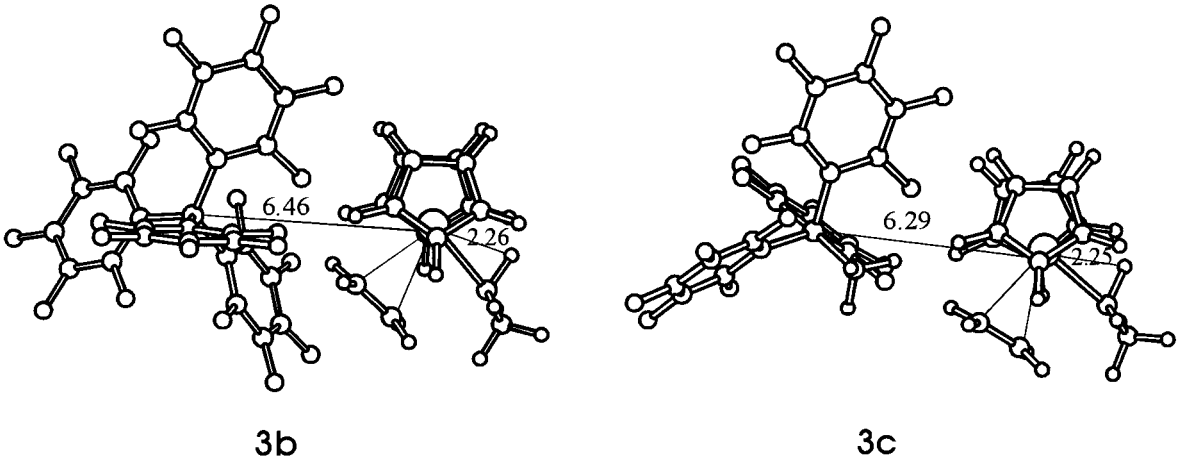

Figure 9. Structures of the complexes **3b,c**.

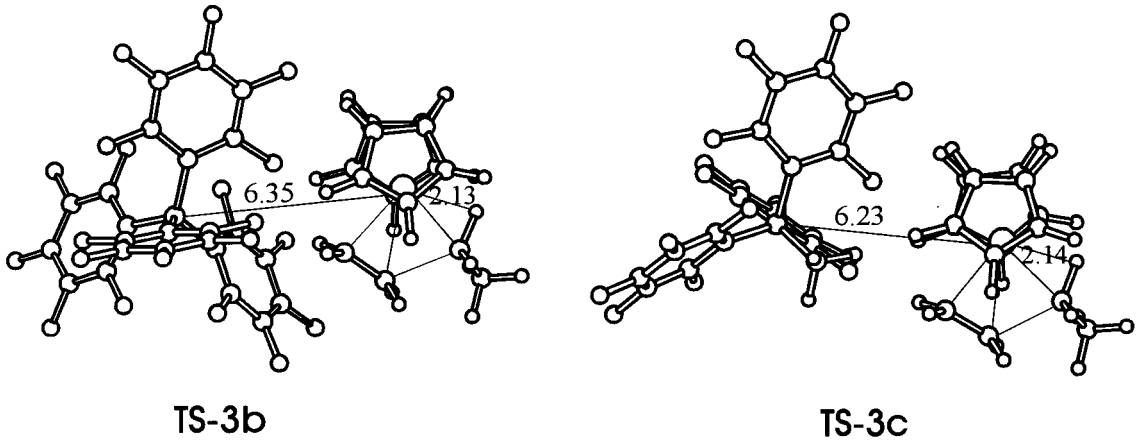

Figure 10. Structures of the transition states **TS-3b,c**.

complex **3a** (Figure 11) was obtained by point-by-point scanning the PES of the system under study when moving along the reaction coordinate.

As in the case of ethylzirconocene cation, the energy barriers **TS-3b,c** to the transformations **3b,c** → **4b,c** in the systems $Cp_2ZrEt^+A^-$ are low (the energy differences between **TS-3b,c** and **3b,c** do not exceed 2 kcal/mol). The energies of the transition states **TS-3b,c** and **TS-2b,c** calculated relative to those of noninteracting reagents (**1a**−**c** + C_2H_4) are of the same order of magnitude, the former being somewhat higher.

As can be seen in Figure 12, the structures of γ-agostic complexes **4a**−**c** differ in Zr—H_{agost} distance and, hence, in strength of the γ-agostic bond. The strongest γ-agostic bond among the complexes **4** is formed in the ethylzirconocene cation **4a** (2.21 Å). In the ion pairs **4b,c**, the γ-agostic bond weakens appreciably since it is involved in competition with the anion in the coordination sphere of Zr. Nevertheless, it is remarkable to note that the strength of the agostic bond in **TS-3** (Zr—H_{agost} distance in both **TS-3b** and **TS-3c** is 2.13 Å) remains higher than that in **3** and **4**.

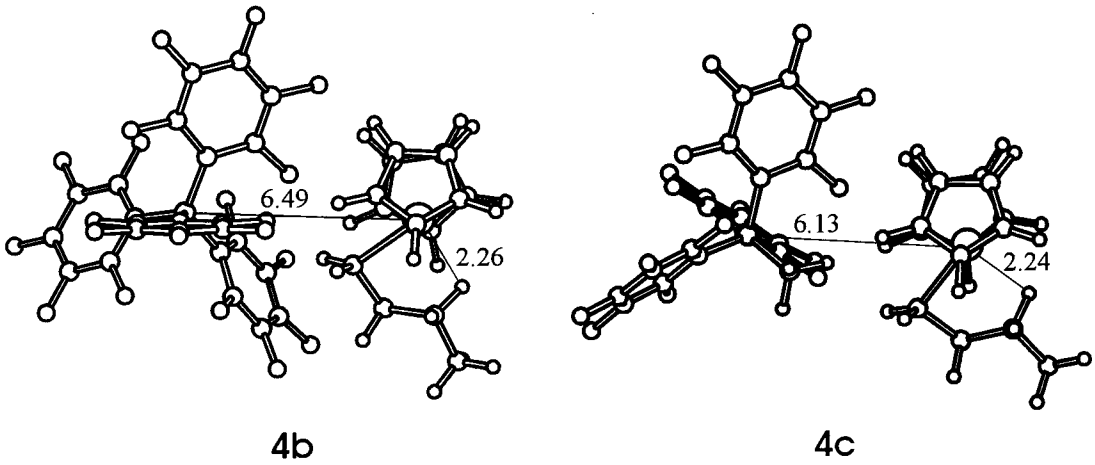

Figure 11. Structures of the complexes **4b,c**.

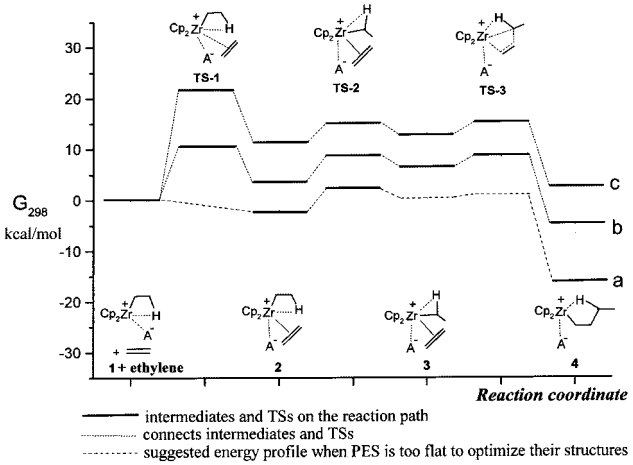

Figure 12. Free energy profile for the complexes **1** interaction with C_2H_4.

Thus, we succeeded to localize the intermediates **2**−**4** and transition states **TS-1**, **TS-2**, and **TS-3**. The ΔG_{298} values for all intermediates and transition states of the transformation **1** → **4** calculated relative to noninteracting reagents (**1** + C_2H_4) are presented in Figure 12. As can be seen in Figure 12, the free energy, ΔG_{298}, of **TS-1** depends strongly on the interactions within the ion pair. Since the distance between the anion and cation increases appreciably upon the addition of ethylene molecule (Table 3), the bonding within the ion pair weakens. This leads to two important consequences, namely, (i) an increase in the energy barrier to be overcome by the system in the order ethylzirconocene cation < $B(C_6F_5)_4^-$ < $CH_3B(C_6F_5)_3^-$ and (ii) an increase in the relative energy, ΔG_{298}, of the addition product **2**.

The energies of transition states **TS-1** in these systems are mainly determined by nucleophilicity of the anion A^-. The higher the nucleophilicity of the anion A^-, the higher the energy barrier to the ethylene addition and the larger the ΔG_{298} value for this reaction.

We found that the free activation energies for the second and third reaction stages (Scheme 2), i.e., the differences between the Gibbs free energies, G_{298}, of **TS-2** and **TS-3** and the corresponding intermediates **2** and **3** depend slightly on the nature of the system. The free activation energies $G_{298}^{\ddagger} = G_{298}$(**TS-2**) − G_{298}(**2**) are 4.5 (**a**), 4.9 (**b**), and 3.8 kcal/mol (**c**), while $G_{298}^{\ddagger} = G_{298}$(**TS-3**) − G_{298}(**3**) are ∼0 (**a**), 1.9 (**b**), and 2.2 kcal/mol (**c**). This is mainly due to a much lesser change in the Zr—B distance in these reaction stages compared to the first stage. As can be seen from the data listed above, the differences G_{298}(**TS-3**) − G_{298}(**3**) are small compared to the G_{298}(**TS-1**) − G_{298}(**1** + C_2H_4) and G_{298}(**TS-2**) − G_{298}(**2**) values.

Thus, we found that the effect of counterion on the energy profile of the transformation **1** → **4** manifests itself in a decrease in the overall exothermicity of the reaction with increasing the nucleophilicity of the anion (i.e., strengthening of the interaction between the anion and cation). For instance, in the system with A^- = $CH_3B(C_6F_5)_3^-$ the energies of all intermediates and transition states of the reaction calculated relative to noninteracting reagents are higher than in the system with A^- = $B(C_6F_5)_4^-$. The most pronounced exothermal effect was obtained for the reaction with "naked" ethylzirconocene cation. In addition, we found that the energy barrier to the ethylene addition in the systems $Cp_2ZrEt^+A^-$ differs from 0 and can be comparable in magnitude with (for A^- = $B(C_6F_5)_4^-$) or even appreciably higher than (for A^- = $CH_3B(C_6F_5)_3^-$) the energy barrier to isomerization of the β-agostic complex of the type **2** into α-agostic complex **3**. The ratio of the heights of the barriers **TS-1** and **TS-2** is determined solely by nucleophilicity of the anion A^-, i.e., by the energy of the interaction between the anion and cation. The higher the nucleophilicity of the anion, the higher the barrier **TS-1**. The heights of the barriers **TS-2** and **TS-3** calculated relative to **2** and **3**, respectively, depend slightly on the properties of counterion.

(4) Isomerization of Primary Reaction Product 4. γ-Agostic complex **4** formed as a result of the transformations discussed above is characterized by a high degree of charge separation in the ion pair. The corresponding loss of energy cannot be compensated by the weak γ-agostic bond. Therefore, the formation of complex **4** is followed by its isomerization into a more thermodynamically stable compound. This transformation can proceed by several mechanisms presented in Scheme 3, which can be divided into two groups. The first group of mechanisms involves no large-amplitude motions of the anion and cation relative to each other. Here, the transformations themselves are due to the cleavage/formation of agostic bonds and internal rota-

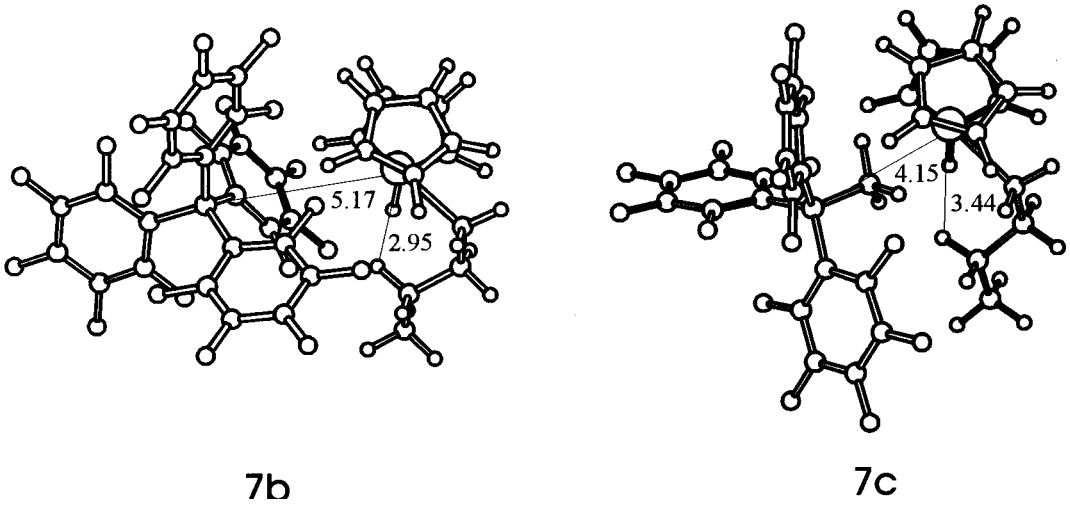

Figure 13. Structures of the complexes **7b,c**.

Scheme 3

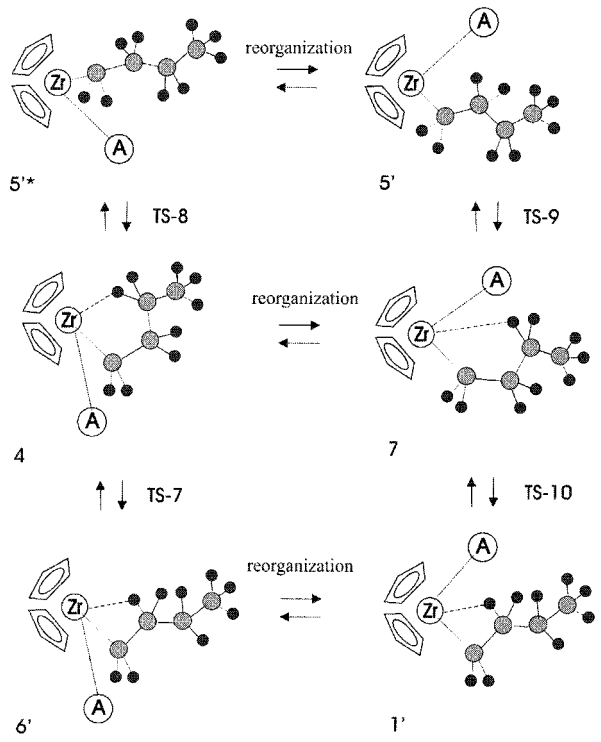

tions (denoted by vertical arrows in Scheme 3). The second group of mechanisms involves the so-called "reorganization", i.e., such a motion of the anion and cation that the system rearranges and the anion appears on the opposite side with respect to the Cp_2ZrBu fragment (denoted by horizontal arrows in Scheme 3). Reorganization can be accompanied by internal rotation about the Zr—C bond and/or by cleavage of the agostic bond.

For systems with "naked" ethylzirconocene cation, the main channel of the transformation of complex **4** is associated with the isomerization of complex **4a** into β-agostic complex **6′** (an analogue of complex **6** with one additional monomer unit) through transition state **TS-7** (Scheme 3). This type of transition state has already been reported by Morokuma et al.[5a] The energy of **TS-7a** is only slightly higher than that of **4a**. In the case of cation **4a** (no anion), this transformation immediately entails the beginning of a new polymerization cycle, since here the structures **1′** and **6′** are exactly the same. In systems with the ion pairs considered as model catalytic species, some other processes are also possible.

The next channel is the transformation of complex **4** into nonagostic complex **5′*** (an analogue of complex **5*** with one additional monomer unit). We optimized the structures of the transition states **TS-8** of this reaction. As in the case of **TS-7**, the energies of **TS-8** differ only slightly from those of complexes **4**. The thermodynamic characteristics of **TS-7** and **TS-8** and those of the products **6′** and **5′*** are listed in Table 3.

Yet another possible channel of the transformation of complex **4** involves its reorganization to give complex **7**. The structures of complexes **7b,c** are shown in Figure 13, and their thermodynamic characteristics are listed in Table 3. As can be seen in Figure 13 and from the data listed in Table 3, the weak γ-agostic bond in complex appears to be cleaved, since the $Zr—H_\gamma$ distance in both cases is longer than the sum of the van der Waals radii. Therefore, the conformation of the butyl fragment is the only feature common to the complex **7** and the γ-agostic complex. Whereas the γ-agostic bond is cleaved as a result of transformation **4** → **7**, the bonding within the ion pair becomes, on the contrary, stronger. This is indicated by the dramatic shortening of the Zr—B distances in complexes **7b** and **7c** compared to the corresponding distances in structures **4b** and **4c** (by 1.3 and 2.0 Å, respectively!). This makes the reorganization extremely energetically favorable. For instance, the ΔG_{298} values for the transformations **4b** → **7b** ($A^- = B(C_6F_5)_4^-$) and **4c** → **7c** ($A^- = CH_3B(C_6F_5)_3^-$) are −8.3 and −19.0 kcal/mol, respectively.

We failed to find the transition state of reorganization **4** → **7**. Since the system comprises two fragments bound by weak interactions, the search for transition states of their rearrangements is a rather complicated problem due to a slight dependence of the energy of the system on geometric parameters in the region of transition states. In addition, the role of solvation effects in these processes is of prime importance, since they can lead to substantial differences between the true reorganization energies and those calculated for the gas phase.

Previously, Marks et al.[23] carried out detailed studies of reorganization of $[(1,2\text{-}Me_2Cp)_2ZrMe]^+[MeB(C_6F_5)_3]^-$

and estimated the $\Delta G^{\ddagger}_{reorg}$ value for this system at nearly 18−20 kcal/mol at 25 °C in toluene. It is of great importance to note that they considered a degenerate (i.e., thermally neutral) process. The fundamental difference of the systems studied in this work is that the energy of complex **7** is much lower than that of **4** (e.g., $\Delta G = G(\mathbf{7c}) - G(\mathbf{4c}) = -19.3$ kcal/mol). The energy gain obtained in this case nearly coincides with the height of the barrier (20 kcal/mol) measured by Marks et al.[23] This indicates that the height of the energy barrier to the reorganization **4** → **7** is much lower than that measured for $[(1,2\text{-}Me_2Cp)_2ZrMe]^+[MeB(C_6F_5)_3]^-$ and may be lower than **TS-7** and **TS-8** (only in that case one can observe a chain-migration mechanism!).

As can be seen in Scheme 3, the formation of complexes **5′*** and **6′** can also be followed by reorganization (Scheme 3), which results in complexes **5′** and **1′**, respectively. Nevertheless, the structure **4** seems to be the most appropriate for the reorganization to occur since (i) it has the longest Zr−B distance and, hence, is the "loosest" ion pair and (ii) it is the reorganization of complex **4** that is characterized by the highest exothermicity. Based on the aforesaid, the most probable mechanism of γ-complex isomerization involves reorganization **4** → **7** followed by transformation of complex **7** into either **5′** (relaxation of γ-agostic complex **4** results in complex **5′** rather than **5′*** as the kinetic product) or β-agostic complex **1′** by internal rotations about the Zr−C and C−C bonds of the butyl fragment.

Analysis of the data listed in Table 3 showed that the energy of complex **7** is not too high compared to those of **1′** and **5′**. Structurally, complex **7** is very similar to **5′** and can undergo a ready rearrangement to give the latter by internal rotation about the Zr−C bond and the C−C bond of the butyl fragment. The energy barrier **TS-9** associated with this transformation either is low (**TS-9b**) or nearly equals zero (**TS-9c**). The second channel of transformations involves the formation of β-agostic complex **1′**; however, it seems to be less probable for the following reasons. Like the complex **1c** considered in part I, the energy of its analogue **1′c** is higher than that of complex **5′c**. The difference of free Gibbs energies of β-agostic isomer **1b** and nonagostic isomer **5b** is negligible and decreases from $\Delta G_{298}(\mathbf{1b}) - \Delta G_{298}(\mathbf{5b}) = 0.9$ kcal/mol to $\Delta G_{298}(\mathbf{1'b}) - \Delta G_{298}(\mathbf{5'b}) = 0.4$ kcal/mol with polymer chain growth. This is likely due to the mutual steric repulsion between the butyl fragment (i.e., the growing polymer chain) and counterion in complex **1′b**.

Transformation **7c** → **5′c** is energetically more favorable than **7c** → **1′c** since the energy barrier is higher for the second process and the energy of complex **5′c** is lower than that of **1′c**. Thus, the results obtained in this work indicate that the most probable channel of transformation of intermediate complex **7c** involves its rearrangement into nonagostic complex **5′c**. For the complex **7b** both channels **7b** → **1′b** and **7b** → **5′b** are probable. In this connection, the problem of the resting state of the catalytic species takes on great significance. We can assume that not only the β-agostic isomer **1** but also nonagostic isomer **5** can be the resting state of the catalyst.

Complex **5*** is a conformer of complex **5**. Analogously, there exists a complex **5′***, which is a conformer of complex **5′**. Comparison of the energies of the four complexes of the type **5** for two counterions considered (see Tables 1 and 3) reveals insignificant energy differences between the conformers **5** and **5*** (**5′** and **5′***). It does not always happen that conformer **5*** (**5′***) is the most thermodynamically stable. If the growing polymer chain is represented as ethyl fragment, the energy of conformer **5*c** is lower than that of **5c**; however, in the case of chain extension even by one unit (i.e., if the growing polymer chain is represented as the butyl fragment) the energy of **5′c** appears to be appreciably lower than that of **5′*c**.

Table 4. Thermodynamic Data of the Intermediates and Transition States for the Chain Termination Reaction 2 → 8

	for given param[a]			
	E, kcal/mol	H_{298}, kcal/mol	G_{298}, kcal/mol	Zr−B, Å
	Naked Cation Cp_2ZrEt^+			
1a	0	0	0	
2a (**8a**)	16.2	14.4	2.0	
TS-11a	8.0	8.6	5.6	
	$A^- = B(C_6F_5)_4^-$			
1b	0	0	0	5.19
2b	9.6	7.2	3.8	6.65
TS-11b	3.6	3.2	15.6	6.62
8b	6.2	4.3	7.3	6.55
	$A^- = CH_3B(C_6F_5)_3^-$			
1c	0	0	0	4.36
2c	1.0	0.1	11.3	6.68
TS-11c	8.8	7.4	20.6	6.47
8c	2.1	3.3	15.4	6.50

[a] Energies (*E*), enthalpies (H_{298}), and Gibbs free energies (G_{298}) are given relative to the corresponding values for noninteracting reagents **1** + C_2H_4.

(5) Chain Termination. Ziegler et al.[7c] reported a detailed comparison of three possible mechanisms for chain termination in the system $Cp_2ZrEt^+ + C_2H_4$ and found that the most probable mechanism involves an intrasphere migration of the β-agostic H atom in intermediate **2** from the alkyl fragment (the growing polymer chain) to the coordinated ethylene molecule. Therefore, in this work we considered only the process dealing with β-hydrogen shift:

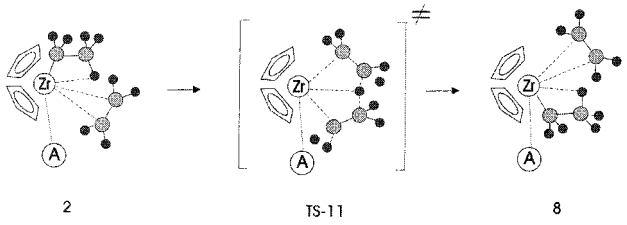

We will not dwell on the other two mechanisms in this study, since our calculations of the energy profiles of these processes showed that they are even less probable in the systems with ion pairs than in the system with "naked" cation.

In the absence of anion (a system with Cp_2ZrEt^+ cation), the structures **2** and **8** are exactly the same. The energies and thermodynamic characteristics of complexes **2** and **8** and transition state **TS-11** are listed in Table 4. The structures of transition state **TS-11** and complex **8** are shown in Figures 14 and 15, respectively. Unlike the structure of **TS-11a**, those of

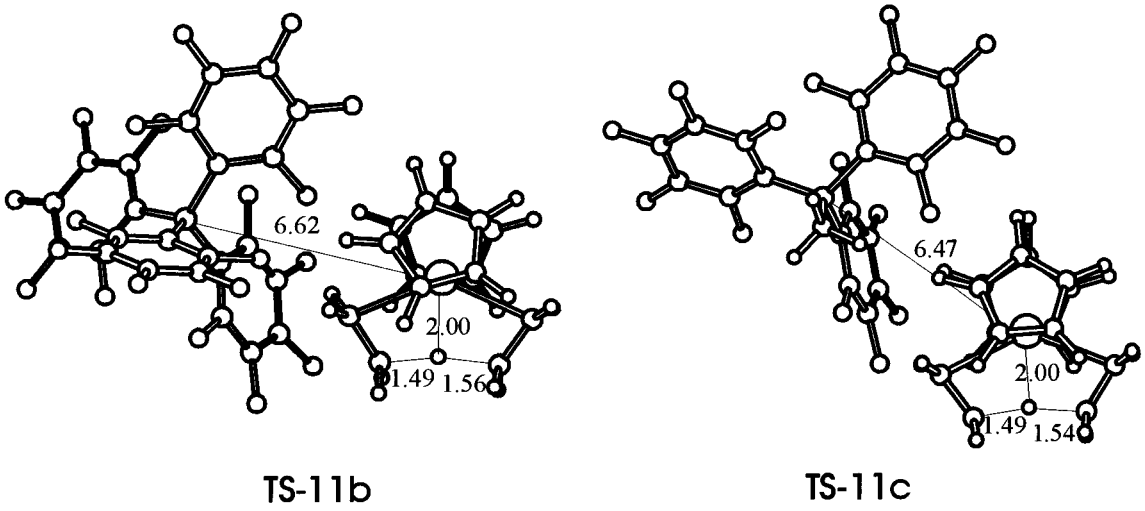

Figure 14. Structures of the transition states **TS-11b,c**.

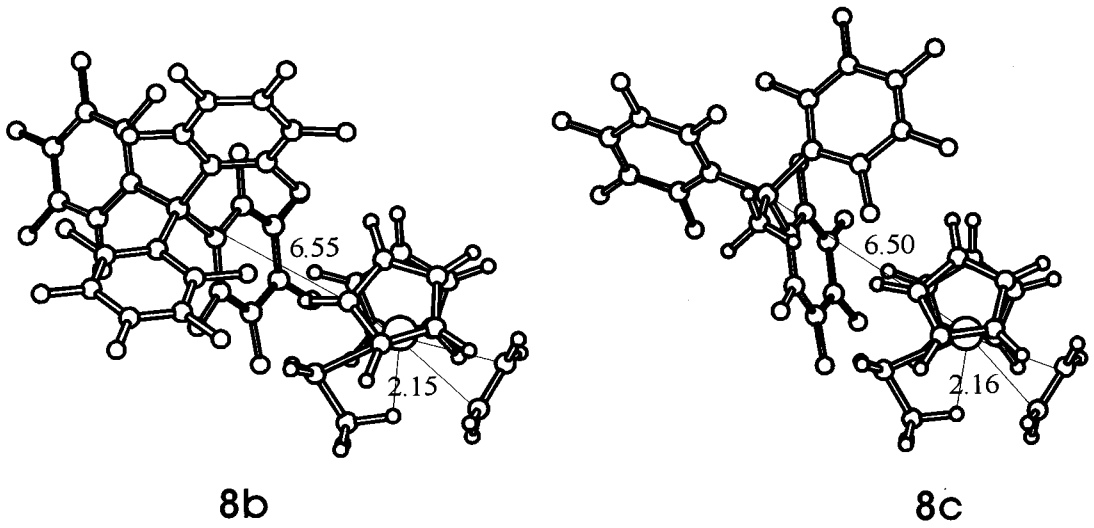

Figure 15. Structures of the complexes **8b,c**.

transition states **TS-11b** and **TS-11c** are asymmetric (see Figure 14) and lie somewhat closer to the reaction product **8** rather than the initial complex **2** on the reaction coordinate. The energies and free energies of complexes **8b** and **8c** are somewhat higher than those of the corresponding complexes **2b** and **2c**. The differences between the free energies of reagents and products are as follows: G_{298}(**8b**) − G_{298}(**2b**) = 3.5 kcal/mol and G_{298}(**8c**) − G_{298}(**2c**) = 4.1 kcal/mol and the free activation energies are G_{298}(**TS-11b**) − G_{298}(**2b**) = 11.8 kcal/mol and G_{298}(**TS-11c**) − G_{298}(**2c**) = 11.3 kcal/mol. Since in the system with ethylzirconocene cation the reaction is thermally neutral, the free activation energy is somewhat lower: G_{298}(**TS-11a**) − G_{298}(**2a**) = 7.6 kcal/mol.

The results obtained show that changes in the nucleophilicity of counterion have no pronounced effect on the height of the energy barrier **TS-11** relative to **2**. This suggests that the interaction with the counterion affects only slightly the energetics of chain termination.

(III) Alternative Reaction Channels. (A) Other Mechanisms of Ethylene Addition to Complexes 1, 5, and 6. As was mentioned above, the energy barrier to the addition of ethylene molecule (**TS-1**) can be comparable in magnitude or even higher than other barriers on the reaction pathway (**TS-2** and **TS-3**). We consider in detail all possible pathways of ethylene addition to complexes **1**, **5**, and **6** taking the system $Cp_2ZrEt^+A^-$ with $A^- = CH_3B(C_6F_5)_3^-$ as an example. Compared to other systems, in this case the energy of complex **5** is lower than that of **1** and, hence, some of new pathways and corresponding mechanisms can be of crucial importance.

These mechanisms are illustrated in Scheme 4. The structures of corresponding transition states, **TS-12**−**TS-19**, of the addition of ethylene molecule to complexes **1**, **5**, and **6** are shown in Figure 16 and their thermodynamic characteristics are listed in Table 5.

Generally, the addition of ethylene molecule to isomers **1**, **5**, and **6** can proceed following two different directions, namely, from the front side or from the backside. In turn, there are two manners for the front-side addition to occur. The ethylene molecule can, first, be oriented perpendicular or nearly perpendicular to the plane, which passes through the Zr atom and is equidistant from the cyclopentadienyl ligands (hereafter, front-perpendicular addition), and, second, be in or deviate only slightly from this plane (hereafter, front-normal addition). The possibility for the front-perpen-

Scheme 4

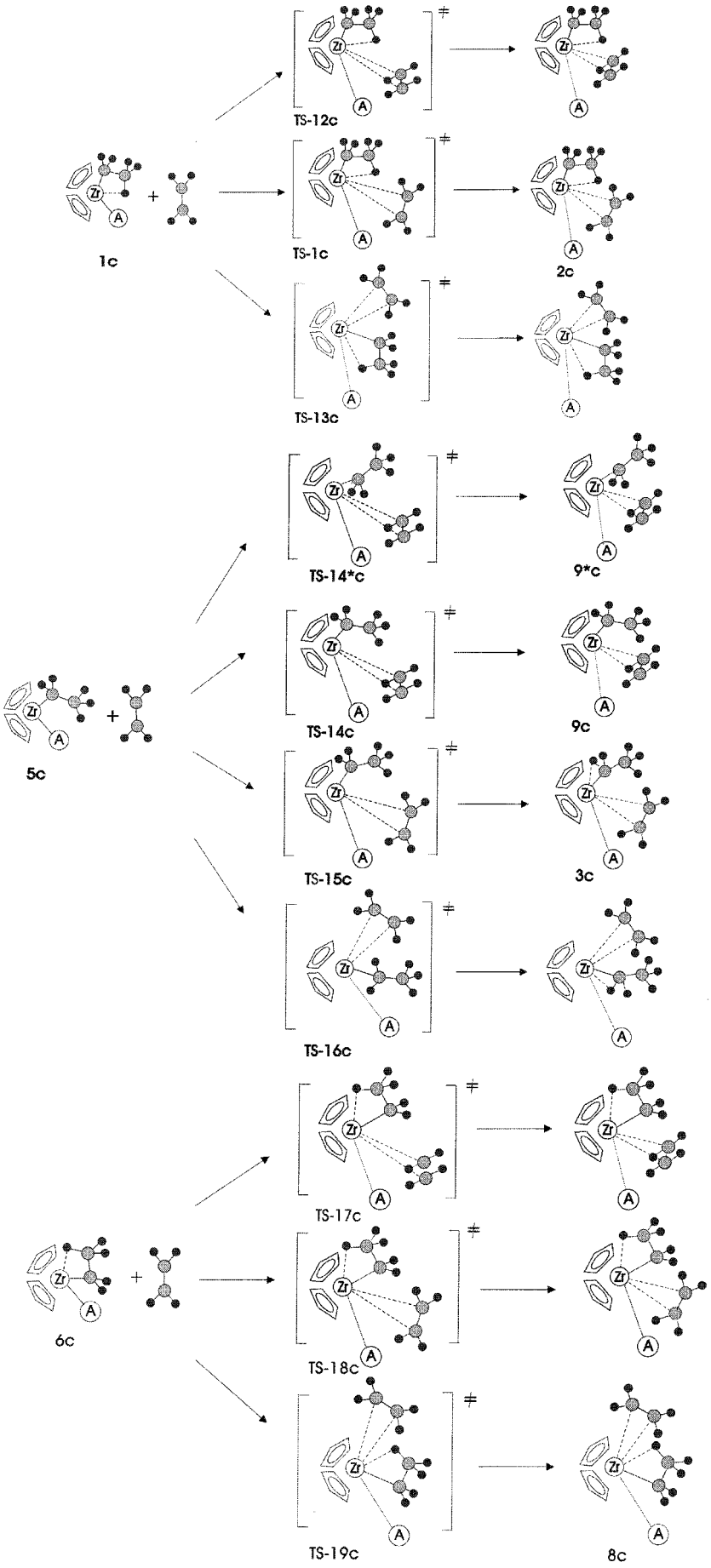

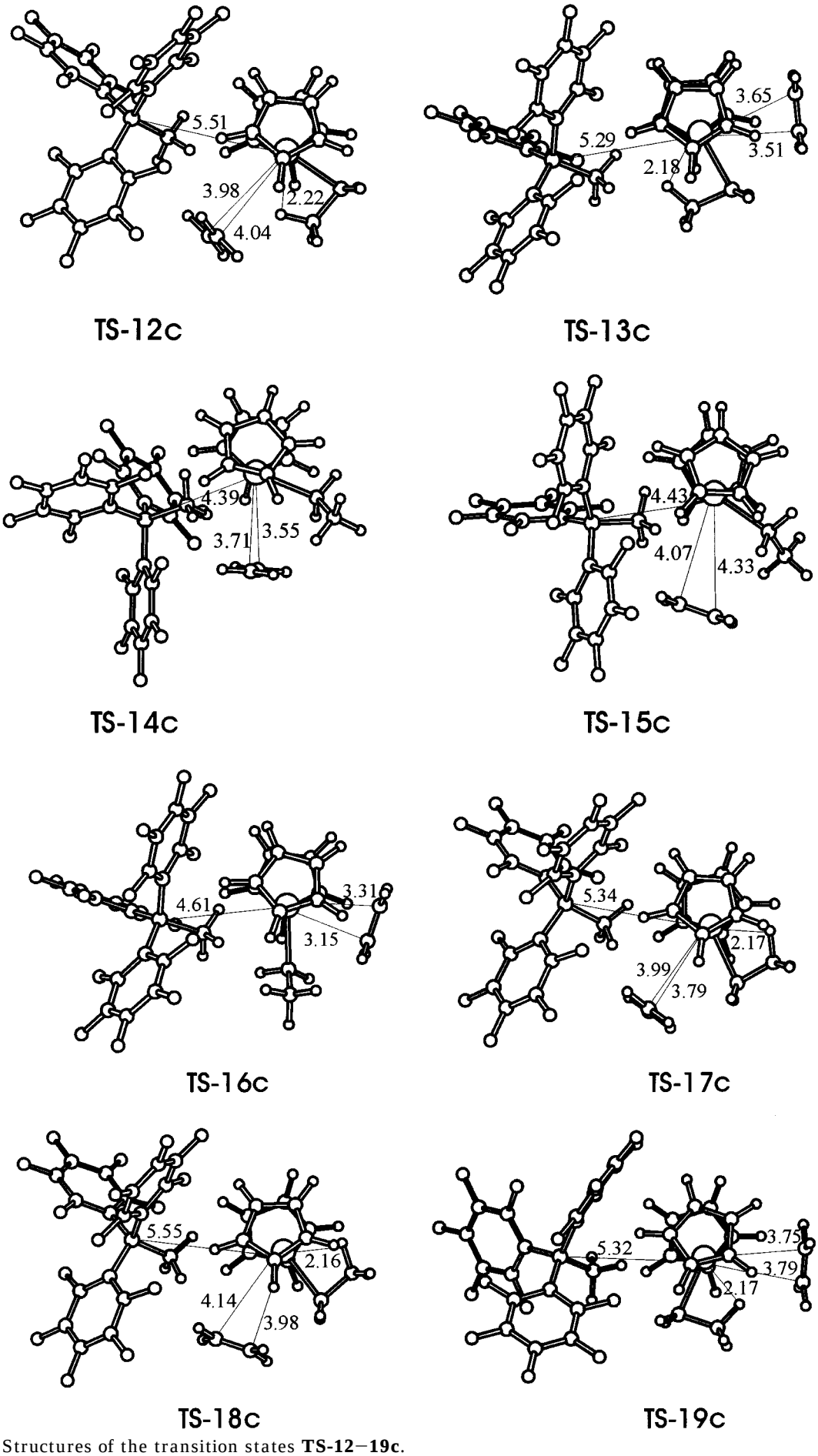

Figure 16. Structures of the transition states **TS-12**−**19c**.

Table 5. Thermodynamic Data for Transition States of the Ethylene Addition to Different Isomers of the Model Catalytic Species $Cp_2ZrEt^+CH_3(C_6F_5)_3^-$

	for given param[a]							
	starting isomer	ethylene addition direction	E, kcal/mol	H_{298}, kcal/mol	G_{298}, kcal/mol	Zr−C (C_2H_4), Å		ZrB, Å
TS-12c	1	front-perpendicular[b]	9.9	10.4	20.3	3.98	4.04	5.51
TS-1c	1	front-normal[c]	10.4	10.6	21.7	4.16	4.53	5.45
TS-13c	1	back	9.5	9.6	20.6	3.51	3.65	5.29
TS-14c	5	front-perpendicular[b]	2.0	3.2	15.8	3.55	3.71	4.39
TS-14*c	5*	front-perpendicular[b]	0.6	1.0	14.2	3.45	3.52	4.38
TS-15c[d]	5	front-normal[c]	8.9	(7.6)	(21.8)	4.07	4.33	4.43
TS-16c	5	back	10.6	11.0	23.2	3.15	3.31	4.61
TS-17c	6	front-perpendicular[b]	12.3	12.5	23.2	3.79	3.99	5.34
TS-18c	6	front-normal[c]	15.1	15.2	25.3	3.98	4.14	5.55
TS-19c	6	back	13.1	12.9	23.1	3.75	3.79	5.32

[a] Energies (E), enthalpies (H_{298}), and Gibbs free energies (G_{298}) are given relative to the corresponding values for noninteracting reagents **1c** + C_2H_4. [b] The ethylene molecule is oriented perpendicular to the plane equidistant with respect to the Cp ligands [c] The ethylene molecule is in the plane which is equidistant from Cp ligands. [d] **TS-15c** is not fully optimized structure.

Scheme 5

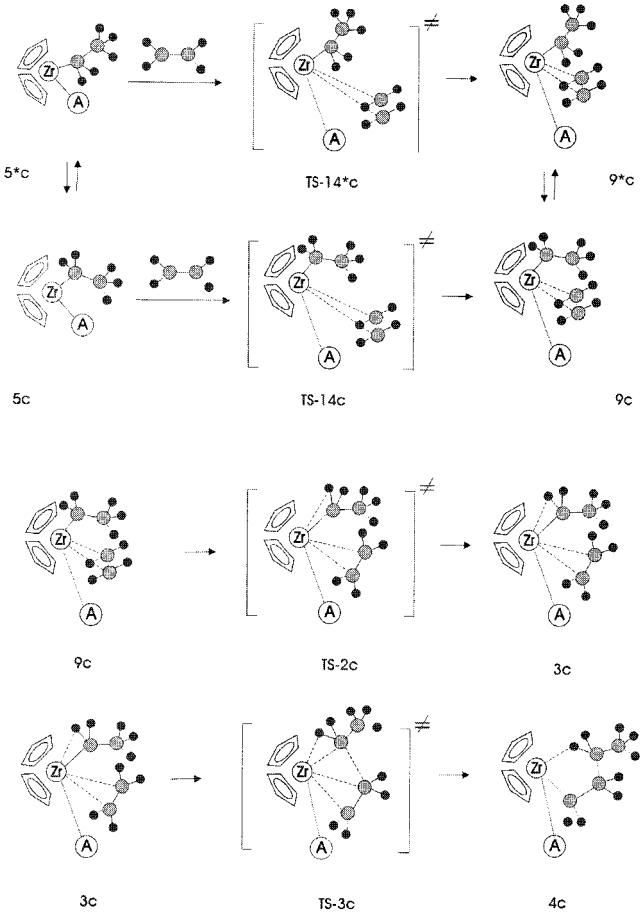

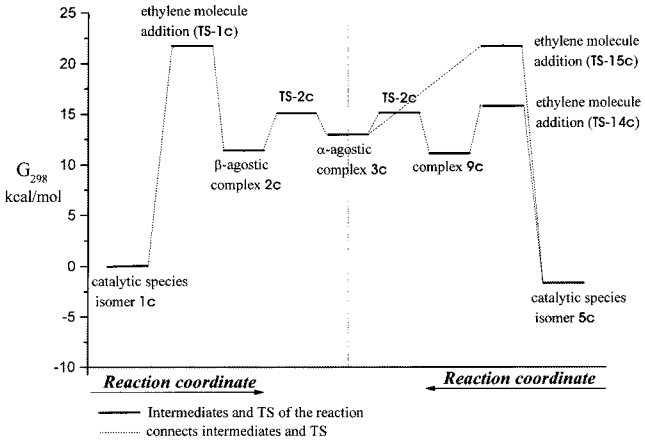

Figure 17. Free energy profile for the complex **3c** formation from isomers **1c** and **5c** and ethylene molecule.

dicular addition of the ethylene molecule to occur was shown in our previous study[15] taking ethylzirconocene cation as an example. In this case, steric hindrances produced by the anion make this mechanism even more energetically favorable than front-normal addition.

As follows from the data listed in Table 5, transition states **TS-14c** and **TS-14*c** of the reaction of ethylene addition to complexes **5c** and **5*c** have the lowest energies. Similarly to the existence of complex **5*c**, which is a conformer of complex **5c**, different conformers of transition state **TS-14c** (e.g., **TS-14*c**) can also exist. Transition states **TS-14c** and **TS-14*c** differ in the angle of rotation of the ethyl unit with respect to the Cp_2Zr fragment. We found that the energy differences between transition states **TS-14c** and **TS-14*c** of ethylene addition to **5c** and **5*c**, respectively, are insignificant (Table 5), which is similar to the situation with the conformers **5c** and **5*c** (see above). However, the energy barriers **TS-14c** and **TS-14*c** are still rather high compared to **5c** and **5*c**, respectively. The corresponding free activation energies of ethylene addition to **5c** and **5*c** are equal to 17.5 and 16.3 kcal/mol, respectively.

Dynamic NMR studies[24] on the *intramolecular* complexation between the zirconocene and ethylene fragments showed that, depending on the type of the system under study, the addition of ethylene molecule is characterized by a $\Delta G_{298}^{\ddagger}$ value of the order of at least 10 kcal/mol (in dichloromethane). This indicates that the barrier to addition does exist. The experimental estimates of the barrier height[24] are of the same order of magnitude as the $\Delta G_{298}^{\ddagger}$ values calculated in this work.

It is noteworthy that out of the two directions of addition (front-perpendicular, **TS-14c**, and front-normal, **TS-15c**) the former is the most energetically favorable. The search for **TS-15c** in the system under study ($A^- = CH_3B(C_6F_5)_3^-$) presents great difficulties since the ethylene molecule tends to rotation to take up a perpendicular position, so that this transition state can be found only by point-by-point scanning the PES of the

(24) (a) Casey, Ch. P.; Carpenetti, D. W., II.; Sakurai, H. *J. Am. Chem. Soc.* **1999**, *121*, 9483. (b) Casey, Ch. P.; Carpenetti, D. W., II. *Organometallics* **2000**, *19*, 3970.

system. Therefore, the estimates of thermodynamic parameters of this transition state listed in Table 5 should be regarded as rough approximation.

Front-side addition of ethylene molecule to isomer **5c** results in complex **9c** (Scheme 5). The Gibbs free energy, G_{298}(**9c**), of this complex calculated relative to those of noninteracting reagents **1** + C_2H_4 is 11.6 kcal/mol. Analogously, ethylene addition to conformer **5*c** results in complex **9*c** with the slightly higher (by 1.4 kcal/mol) Gibbs free energy compared to **9c**. Similarly to conversion of **5c** into **5c***, complex **9c** can be readily converted into **9c*** by rotating the ethyl fragment about the Zr—C bond.

After front-side addition to complex **5c** the ethylene molecule rotates in the coordination sphere of the Zr ion by 90°. Point-by-point scanning the dependence of the energy of the system on the angle of rotation of the ethylene molecule showed that the energy increases monotonically as the angle of rotation approaches 90°. In this range of angles the rotation of ethylene molecule is accompanied by the formation of α-agostic bond, which proceeds through transition state **TS-2c** (for details, see section "Isomerization of *β*-Agostic Intermediate **2** into α-Agostic Complex **3**", part II(A)(2)).

The mechanisms involving front-perpendicular addition of ethylene molecule followed by its rotation by about 90° within the transition-metal coordination sphere have been studied previously taking model homogeneous[5c] and heterogeneous[13] catalysts as examples.

Comparison of the reactions mechanisms shown in Schemes 2 and 5 suggests that they differ only in the first two stages. It is noteworthy that the second stage of the isomerization of the ethylene complexes (**2** or **9c**, respectively) results in the intermediate **3**, which appears to be common to both mechanisms and undergoes then the same transformations. Of particular importance is the fact that the transformation of intermediate **9c** into transition state **TS-2c** proceeds smoothly and is not accompanied by the formation of new intermediate complexes or transition states. This is confirmed by the relaxation of **TS-2c** into the intermediate **9c** upon geometry optimization without any restrictions imposed on geometric parameters.

The energy profiles of transformations of the isomers **1c** (from left to right) and **5c** (from right to left) into α-agostic complex **3c** are presented in Figure 17. The energy profile of the reaction channel that involves the overcoming of the energy barrier **TS-14*c** is not shown in Figure 17, since it differs only slightly from the corresponding energy profile for **TS-14c** and intermediate **3c** is common to both mechanisms. As can be seen, the maximum energy barrier for the mechanism analogous to that proposed by Ziegler et al. for the "naked" cation[7a−e] is much higher than that for the alternative reaction mechanism proposed in this work (Scheme 5).

Thus, we showed that in the system with the counterion $A^- = CH_3B(C_6F_5)_3^-$ there is at least one reaction channel, for which the activation energy of ethylene addition is lower than for the mechanism considered above (see section "Transformations of Intermediate **1**", part II(A)). We attempted to find the transition states **TS-14b** and **TS-15b** in order to compare the heights of these energy barriers with that of **TS-1b**; however, this attempt failed. Presumably, this can be rationalized assuming that these barriers are even lower than the height of **TS-1b**. It can be assumed that in the system with $A^- = B(C_6F_5)_4^-$ the reaction will also proceed by other mechanisms which are different from that shown in Scheme 2.

Recently, Ziegler et al.[7h] have reported a study on ethylene addition to the $Cp_2ZrEt^+CH_3B(C_6F_5)_3^-$ ion pair. However, they have considered only one reaction channel, namely, the back ethylene attack (in this work, the corresponding reaction channel involves the overcoming of the energy barrier **TS-16c**). No other directions of ethylene addition have been considered in the paper cited.[7h] On the other hand, in this work we studied and compared *all* possible pathways of ethylene addition to the $Cp_2ZrMe^+CH_3B(C_6F_5)_3^-$ ion pair and showed that back ethylene addition is much less energetically favorable than front ethylene attack.

One can adduce some arguments to substantiate preferableness of the front ethylene attack: for *ansa*-compounds including those zirconocenes for which the geometry of Cp_2Zr is similar to that of nonbridged Cp_2Zr fragment (e.g., ethylene-bridged zirconocenes), the back ethylene attack is sterically hindered (probably, even impossible) due to the repulsion between the bridge and the monomer to be added; Lee et al.[25] have studied the interaction of $\{Cp^*_2ZrH_2\}_2$ and $\{Me_2Si(Cp^*)_2ZrH_2\}_2$ with such nucleophiles as PMe_3 anf THF (X-ray diffraction and NMR studies showed that both nucleophiles are added *from the front side*); if ethylene addition does occur from the backside, it remains unclear what is the driving force of chain migration in the course of polymerization.

Using the results obtained, we can estimate the free energies of activation of chain propagation in the case of gas-phase ethylene polymerization on the catalytic species $Cp_2ZrP^+CH_3B(C_6F_5)_3^-$ and $Cp_2ZrP^+B(C_6F_5)_4^-$. We assume that the differences between the Gibbs free energies of the highest energy barrier on the reaction pathway (**TS-3**) and those of free reagents $Cp_2ZrEt^+A^-$ + C_2H_4 (here, $Cp_2ZrEt^+A^-$ is meant the lowest-energy isomer, i.e., **1b** for $A^- = B(C_6F_5)_4^-$ and **5c*** for $A^- = CH_3B(C_6F_5)_3^-$) can serve as such estimates. On the basis of comparison of the corresponding numerical values (9.4 kcal/mol for $A^- = B(C_6F_5)_4^-$ and 17.1 kcal/mol for $A^- = CH_3B(C_6F_5)_3^-$), we can suggest that the gas-phase catalytic activity of the zirconocene catalyst with the $B(C_6F_5)_4^-$ counterion will be higher than that of the catalyst with the $CH_3B(C_6F_5)_3^-$ counterion. This is consistent with the results of experimental studies of the catalytic activities of $Cp_2ZrMe^+B(C_6F_5)_4^-$ and $Cp_2ZrMe^+CH_3B(C_6F_5)_3^-$ in toluene.[18b]

It seems likely that polymerization in a real catalytic system can follow several pathways simultaneously. The results obtained in this work suggest that the "non-agostic" reaction channels (i.e., those for which the stabilization of intermediates and transition states is due to the stronger interaction within the ion pair rather than the formation of *β*-agostic bonds) must be growing in importance with increasing of the nucleophilicity of the counterion. It seems likely that, irrespective of the predominant reaction channel, the reaction pathway always passes through the transition states **TS-2** and

(25) Lee, H.; Destrosiers, P. J.; Gusei, I.; Rheingold, A. L.; Parkin, G. *J. Am. Chem. Soc.* **1998**, *120*, 3255.

TS-3 and the kinetics of the overall process is controlled by the ability of the system to overcome these two energy barriers.

The results obtained in the present study make possible estimation of the molecular weight of polyethylene formed on catalytic species $Cp_2ZrP^+A^-$ (here, P = is the growing polymer chain and $A^- = B(C_6F_5)_4^-$ or $CH_3B(C_6F_5)_3^-$)). This can be done using the difference between the free energies of transition states of chain termination (**TS-11**) and chain propagation (**TS-3**)[7c] and ethyl group to represent the growing polymer chain. According to our calculations, the energy differences are 6.2 kcal/mol for $A^- = B(C_6F_5)_4^-$ and 5.3 kcal/mol for $A^- = CH_3B(C_6F_5)_3^-$ (for $T = 298$ K). The expected values of the molecular weight of polyethylene obtained using the Maxwell−Boltzmann formula are 200 000 g/mol for $Cp_2ZrMe^+CH_3B(C_6F_5)_3^-$ and 1000 000 g/mol for $Cp_2ZrMe^+B(C_6F_5)_4^-$ (both for $T = 298$ K). Taking into account that the distances between the components of the ion pairs in transition states **TS-11** and **TS-3** differ insignificantly, the ratio of the Gibbs free energies of **TS-11** and **TS-3** in a low-polar solvent (e.g., toluene) should not radically change as compared to the gas-phase reaction. Therefore, this estimate of the molecular weight of polyethylene will also be realistic for ethylene polymerization in toluene; the corresponding experimental data are available in the literature. Marks et al. have found that the molecular weight of polyethylene formed on the $Cp_2ZrMe^+CH_3B(C_6F_5)_3^-$ and $Cp_2ZrMe^+B(C_6F_5)_4^-$ catalysts (25 °C, toluene) is 124 000 and 987 000 g/mol, respectively.[18b] This is in satisfactory agreement with our estimates.

Conclusion

In this work, we studied the mechanism and energy characteristics of a model process of ethylene polymerization on zirconocene catalysts and showed that the use of the ion pairs $Cp_2ZrEt^+A^-$ and Cp_2ZrEt^+ cation as model catalysts lead to *essentially* different results. This is due to the fact that the energy of the interaction between counterions within the ion pair, assessed from changes in the Zr—B distance, differs for the intermediates and transition states of ethylene polymerization. The effect of counterion manifests itself to the greatest extent in the stage of addition of ethylene molecule to the ion pair **1**. Depending on the type of anion, the Zr—B distance increases by 1.1—1.2 Å in the transition state **TS-1** and by 1.5—2.3 Å in the reaction product **2**. The addition of ethylene molecule to the ion pair **5c** leads to a much smaller increase in the Zr—B distance in the transition states **TS-14c** and **TS-15c** (by 0.24 and 0.28 Å, respectively), though in the addition products **3c** and **9c** this distance increases by 1.6—2.2 Å compared to complex **5c**. Therefore, both kinetic and thermodynamic parameters of the stage of ethylene addition are strongly dependent on the nucleophilic properties of the counterion. The most energetically favorable pathway of ethylene addition involves the overcoming of transition state **TS-14** since in this case changes in the Zr—B distance are minimum. On the other hand, insignificant changes in the Zr—B distance upon the isomerization of ethylene complexes **2** → **4** indicate that the nature of counterion has little effect on this process.

The results obtained in the present study are sufficient to allow some assumptions of the methods for controlling the activity of metallocene catalysts. Apparently, it can be enhanced not only by weakening of nucleophilic properties of the counterion (the use of, e.g., weak nucleophilic counterions, high Al/Zr ratios in MAO containing catalytic systems, and polar solvents), but also by a *decrease in positive atomic charge on Zr* by introduction of *electron-donor* substituents into the Cp rings of the zirconocene. This feature had been first remarked by Ewen[26] and then has been confirmed by extensive experimental data.[27] When using MAO as cocatalyst, zirconocenes with donor substituents would be not only highly efficient at the practically used Al/Zr ratios, but also sufficiently active at rather low Al/Zr ratios,[28] since the need of using extremely weak nucleophilic counterions (large excess of MAO) loses its meaning with decreasing the electrophilic properties of the zirconium center.

Acknowledgment. Financial support by Montell B.V. is gratefully acknowledged. The authors express their gratitude to Prof. Yu. A. Ustynyuk for fruitful discussions and help in preparation of this work.

Supporting Information Available: Tables of gas-phase energies and Cartesian coordinates and thermodynamic data of all DFT-optimized structures. This material is available free of charge via the Internet at http://pubs.acs.org.

OM010067A

(26) (a) Ewen, J. A. *Stud. Surf. Sci. Catal.* **1986**, *25*, 271. (b) Ewen, J. A.; Welborn, H. C. Eur. Pat. Appl., 0 129 368 (to Exxon), 1984.

(27) The effect of the positive charge of the metal atom on the activity of metallocene catalysts has been recently studied taking CGM as an example in a paper by: Guo, D.; Yang, X.; Liu, T.; Hu, Y. *Macromol. Theory Simul.* **2001**, *10*, 75. Their conclusions are in agreement with the results obtained in this work.

(28) Nifant'ev, I. E.; Bagrov, V. V. PCT Int. Appl., WO9924446 (to Montell), 1999. Luttikhedde, H, Naesman, J.; Leino, R.; Wilen, C.-E. PCT Int. Appl., WO9728170 (to Borealis), 1997.